Ab Initio Composite Approaches for Heavy Element Energetics: Ionization Potentials for the Actinide Series of Elements

Sasha C. North[1] and Angela K. Wilson[2]

[1,2]*Department of Chemistry, Michigan State University, East Lansing, MI 48824*
Correspondence to: Angela K. Wilson (akwilson@msu.edu)

The gas-phase first, second, and third ionization potentials have been determined for the actinide series of elements using an *ab initio* composite scalar and fully relativistic approach, employing the coupled cluster with single, double, and perturbative triple excitations (CCSD(T)) and Dirac Hartree-Fock (DHF) methods, extrapolated to the complete basis set (CBS) limit. The impact of electron correlation and basis set choice within this framework are examined. Additionally, the first three ionization potentials were obtained using an *ab initio* heavy element correlation consistent Composite Approach (here referred to as α-ccCA). This is the first utilization of a ccCA for actinide species.

Keywords: Heavy elements, ionization potentials, *ab initio* methods, composite methods, ccCA

Introduction

The importance of actinides are evident from their applications ranging from nuclear fission reactions to harness nuclear power for the military decades ago to more common use in nuclear power plants [1], providing routes to curb carbon emissions [2–4]. Their curative uses include actinium in the form of actinium-225 as a label for targeted alpha therapy to treat cancer [5–7]. Among the everyday uses of actinides, americium-241 is utilized in ionization smoke detectors [8] and plutonium-238 for cardiac pacemakers. Despite these applications, much of the chemical behavior of the actinides is less known than for main group and transition metal species. A better understanding of the chemistry of actinides will enable new applications, and will optimize current use and waste mitigation strategies for these species

Experimentally, the elements following uranium (Np-Lr) are more difficult to study than the first four elements in the series. In addition to their increasing radioactivity and thus expense and safety protocols for proper handling and maintenance, these species are difficult to study experimentally because the transuranium elements are not naturally occurring. The elements neptunium through fermium have+ been synthesized by neutron bombardment. The later actinides beyond fermium are known to undergo spontaneous fission[9], and thus, their creation involves bombardment of an actinide target with very light nuclei, such as the bombardment of einsteinium-253 with helium atoms to produce mendelevium [10]. The synthesis of these elements is often very slow, and it can take years to produce small amounts. Therefore, available experimental data for the actinide series is quite limited. Thus, computational studies are particularly vital in helping to understand the chemistry of actinide species.

Calculations on heavy element species have been dominated by density functional theory (DFT)[11–14] due to its lower computational cost, relative to *ab initio* methods such as coupled cluster or multireference configuration interaction (MRCI) approaches. However, *ab initio* calculations are important because of the multitude of low-lying electronic states that arise, many of them are near-degenerate from the highly open-shell nature of most of these elements, and from the strong relativistic (mainly spin-orbit) effects that become significant in heavy elements. While DFT has improved vastly since its foundation in the 1960's by Hohenberg and Kohn[15], it is still known to struggle with or fail for highly correlated systems [16,17]. Specifically, overall, DFT has shortcomings in treating static correlation that arises in situations with degeneracy or near-degeneracy [18]; this makes it less than ideal for treating species containing f-elements. Though much work has been done and significant progress has been made towards treating multi-reference systems using DFT[19–29], the efficacy of these methods for f-block elements has not been demonstrated.

Multi-reference methods are typically necessary for the accurate and reliable treatment of non-dynamic correlation effects. However, even internally-contracted MRCI methods [30] become prohibitively expensive for systems with a large number of reference configurations, as is typically needed for the actinides. Identifying single-reference *ab initio* methods that can better (and more reliably and consistently) describe the energetics for these elements than DFT methods, while being less expensive than multi-reference methods, are of tremendous interest.

In terms of less computationally costly approaches, *ab initio* composite methods provide a route to reduce computational cost, while preserving the accuracy of more advanced, albeit, more computationally costly methods. Among the best-known composite methods are the Gaussian-*n* (G*n*)[31–36], Weizmann-*n* (W*n*)[37–40], Complete Basis Set (CBS-*n*)[41–46], High accuracy extrapolated ab initio thermochemistry (HEAT)[47,48], Feller-Peterson-Dixon (FPD)[49–51], and our own correlation consistent

Composite Approach (ccCA)[52–54] approaches. Composite strategies have evolved over several decades, have proven effective, and are widely used for earlier main group species [52–55]. Fewer methods have targeted transition metals; these methods include ccCA from our group which has proven useful [56–58]. ccCA has been extended to the lanthanides but in the early work, utilized the Sapporo basis sets due to the initial unavailability of the correlation consistent basis sets for lanthanides. While the lanthanide composites have been shown to be just as effective with the Sapporo and correlation consistent basis sets, the unique systematic convergence of the correlation consistent basis sets provides superior convergence to the complete basis set (CBS) limit, providing improved reference energies for a composite strategy for the heavy elements [59]. More recently, Peterson[60] and Feng *et al* [61] have developed correlation consistent basis sets for actinides, including the cc-pV*n*Z-DK3 and cc-pwCV*n*Z-DK3 basis sets, contracted using the third-order Douglas-Kroll-Hess (DKH3) Hamiltonian.

For both lanthanides and actinides, as noted, computational studies of energetic properties have been dominated by DFT [62–66]. Recent calculations targeting the Ln54 and An66[67] sets, sets of enthalpies of formation and dissociation energies for lanthanides and actinides with experimental uncertainties of 5 kcal mol^{-1} or less, have assessed the utility of a number of density functionals for heavy element species [68,69]. For lanthanides, the typical errors in the dissociation energies and enthalpies of formation of small molecules are on the order of 1 eV [69]! This performance is not surprising, as available functionals have not been parameterized explicitly for use with heavy elements. Given that the actinides tend to bond more covalently than the lanthanide elements, overall, the errors with respect to experiment when DFT is used are lower on the order of 10 kcal mol^{-1}, on average, for most compounds) than for the lanthanide containing species[67]. In considering and developing routes to improve the prediction of energetics for heavy elements, ionization energies can serve as a useful early gauge of methods, as there are only a handful of molecules which have experimental uncertainties that rival the uncertainties of many hundreds of early main group species.

For lanthanides, prior DFT predictions of ionization energies include fully relativistic DFT (RDFT) [70], and relativistic *ab initio* pseudopotential RDFT [71] calculations. *Ab initio* approaches that have been employed include multi-reference average coupled pair functional (MRACPF) [72], [73], and coupled cluster calculations[73].

In prior work, the third ionization potentials of lanthanides were calculated using the coupled cluster with single, double, and perturbative triple excitations(CCSD(T)) method [74] with non-scalar relativistic effects accounted for using Dirac Hartree Fock calculations. In this prior study, the impact of core correlation and basis set choice were also examined [75]. This CCSD(T)+DHF approach (details given in the computational methods section below) was shown to be effective in modeling lanthanide ionization energies. The use of a scalar relativistic Hamiltonian for the post-Hartree-Fock correlation energy reduced the computational cost relative to a fully relativistic treatment. The fully relativistic Dirac Hartree-Fock method used for treating spin-dependent fully relativistic effects requires a four-component Hamiltonian and significantly increases computational cost. Therefore, accounting for these effects with a separate calculation and adding the resulting contribution to the scalar relativistic effects *a posteriori* provides an efficient and, as shown in the recent lanthanide study, an effective approach at much reduced computational cost.

For actinides, there have been a number of computational studies to investigate methodologies needed to predict atomization energies. Feng and Peterson [61] used the Feller-Peterson-Dixon (FPD) composite approach, based on MRCI+Q energies to calculate the first, second, and third ionization

energies for the actinide series. In an earlier work, Cao and Dolg [76] used complete active space self-consistent field (CASSCF) and multi-reference averaged coupled-pair functional (MRACPF) levels of theory, corrected for spin-orbit interaction, in combination with relativistic energy-consistent small core *ab initio* pseudopotentials (PP) [77,78] to calculate these ionization potentials.

For first ionization energies (IE), the FPD composite approach based on MRCI+Q energies tends to underestimate the IE's by several kcal mol^{-1}. The method predicts second and third ionization energies well within the range of error of experimental values, with uranium the notable exception, as discussed below. The same level of accuracy is achieved for the ionization potentials obtained using the PP-CASSCF/MRACPF method.

In the current study, strategies that were effective for lanthanides (CCSD(T)+DHF) are considered for the actinides, predicting the first, second, and third ionization potentials for the entire actinide series. This is done to determine the potential utility of the strategies for the prediction of actinide ionization potentials in comparison to experiment as well as efficient prediction (i.e., disk space, memory, speed) as compared to multi-reference and fully relativistic methods, as were used in prior studies. The effects of basis set and level of electron correlation (electrons included in the active space) are also examined within the CCSD(T)+DHF framework. In its first use for the actinides, a variant of ccCA, here referred to as α-ccCA, is also introduced and considered.

Computational Methods

I. CCSD(T)+DHF

In this study, scalar relativistic calculations are addressed utilizing CCSD(T) with the third-order Douglas-Kroll-Hess (DKH3) Hamiltonian [79]. For *ab initio* calculations on early main group species, the frozen core approximation is typically used with the default set of valence electrons for the effective prediction of a broad range of properties. For atoms and molecules of the lower periodic table where the electron manifold becomes far more complex due to the increased numbers of electrons and many close-lying electronic states, it is important to consider the impact of a more explicit treatment of the electrons, incorporating a greater number of electrons within the valence space. Thus, in this work, the cc-pV*n*Z-DK3 basis set [61] with *n*=D,T,Q was used for calculations that consider valence electron correlation only.For the actinide series of elements this encompasses electrons in the 6*s*, 6*p*, 5*f*, 7*s* and 6*d* orbitals. The cc-pwCV*n*Z-DK3 basis set [61] was used for two sets of calculations. The first addresses valence electron correlation only and the second includes the orbitals involved in the valence calculation and additionally correlates electrons in the 5*s*, 5*p*, and 5*d* orbitals.

The ionization potential energy is determined as the difference between the energy of the atoms/ions being considered. For example, the second ionization energy is obtained as

$$IP = E(An^{2+}) - E(An^{+}) \quad (1)$$

where *An* is an actinide element.

The total energy for each atom and ion is calculated as shown in equation (2):

$$E_{tot} = E_{ref} + \Delta E_{spin} \quad (2)$$

where E_{ref} is the CCSD(T)-DKH3 scalar relativistic energy. The second term, ΔE_{spin}, accounts for the spin-dependent (vector) relativistic effects in the Dirac Hamiltonian for the electronic energy. This term is calculated as follows:

$$\Delta E_{spin} = E_{DHF} - E_{DHF-SF} \quad (3)$$

and is the difference between the Average-of-Configurations Dirac-Hartree-Fock (AOC- DHF) energy and the spin-free DHF energy [80]. The AOC method [81] as implemented in the DIRAC [82] software package is particularly useful for the optimization of Hartree-Fock orbitals when multiple open subshells lead to many possible fractional occupancies. The Dyall-VTZ basis set [83] was used for all AOC-DHF energy calculations, and was uncontracted for the all-electron relativistic four-component calculations. The triple-ζ level Dyall basis set was chosen based on the prior work which demonstrated [75] that the spin-dependent term was impacted only slightly (< 0.6 kcal mol^{-1} difference) by the choice of basis set level (double-, triple-, or quadruple-ζ) used in ionization potential calculations for the lanthanides; in that work, using the double-ζ level basis set for ΔE_{spin} was found to provide sufficiently accurate results for describing the third ionization energy of the lanthanides with respect to experimental values. Here, the triple-ζ basis set was chosen as a compromise between predicted accuracy and cost in this work. Following the DHF calculation, a Complete Open-Shell Configuration Interaction (COSCI) [84] calculation was done to resolve the energy of the individual states included in the AOC-DHF calculation. From this, the desired electronic state energy was selected.

For a number of the calculations, the CCSD(T)-DKH3 scalar relativistic energies were extrapolated to the CBS limit. For these, the CCSD(T)-DKH3 calculations utilized both the valence and outer core electrons in the valence space, and the cc-pwCV*n*Z-dk3 basis set. The Hartree-Fock energies were extrapolated using the following [85]:

$$E_n = E_\infty + A * e^{(-1.63n)} \quad (4)$$

The first exponential extrapolation scheme was introduced by Feller[8687] and used later by Williams *et al.* to extrapolate Hartree-Fock energies obtained for transition metal diatomics[88]. This approach is a two-point extrapolation, where *n* represents the cardinal number corresponding to the basis set levels used in the CCSD(T)-DKH3 calculations. In the formula, $E\infty$ represents the energy at the CBS limit. The CCSD(T) correlation energies were extrapolated separately, using a series of calculations at the double, triple, and quadruple-ζ level basis set and the following[89]:

$$E_n = E_\infty + A(n + 0.5)^{-4} \quad (5)$$

which has been used previously[90] to extrapolate CCSD(T) correlation energies.

II. α-ccCA composite

The ccCA approach overviewed here is based upon a second-order Møller-Plesset (MP2)[91] reference energy with a number of additional contributions. One contribution accounts for dynamic correlation that is not sufficiently recovered by the MP2 method (ΔE_{cc}). The second contribution, ΔE_{cv}, accounts for core-core and core-valence interactions not treated sufficiently by ΔE_{cc}. Finally, a term accounting for spin-orbit

interactions is included. (Parallel development of ccCA methodology is ongoing for the lanthanides.)).

Overall, the total energy equation is as follows:

$$E_{tot} = E_{ref}(MP2) + \Delta\mathrm{E}cc + \Delta\mathrm{E}cv + \Delta\mathrm{E}_{spin} \qquad (6)$$

For the reference energy, the Hartree-Fock energy and MP2 correlation energy are each separately extrapolated to the CBS limit, and the HF/CBS and MP2/CBS energies are combined to form the reference energy. The CBS limits are based on energies arising from a series of MP2 calculations using the cc-pV*n*Z-DK3 basis set, where *n* is the cardinal number of the basis set (*n*=D,T,Q). Several schemes are considered for the extrapolations (as discussed further in Section III). The considered schemes have been broadly used for earlier portions of the periodic table and have had comparatively limited use for the heavy elements. The formulas used to extrapolate the Hartree-Fock energies include equation (4) and the Karton-Martin formula[92]:

$$E_n = E_\infty + A(n+1)e^{(-6.57\sqrt{n})} \qquad (7)$$

Equation (7) was originally proposed for extrapolation of Hartree-Fock energies, and has also been used more recently to extrapolate complete active space self-consistent field (CASSCF) reference energies obtained for calculation of actinide ionization potentials[61]. The MP2 correlation energy was extrapolated using equation (5) [89], which was also used successfully for the actinides in the study by Feng and Peterson[61]. The MP2 energies were also extrapolated using the mixed Gaussian formula by Peterson, Woon, and Dunning[93],

$$E_n = E_\infty + Ae^{(-(n-1))} + Be^{(-(n-1)^2)} \qquad (8)$$

Equation (8) has been used for the extrapolation of MP2 energies with excellent results in the ccCA and is being employed in several ongoing studies involving ccCA for the heavy elements.

Returning to equation (6), the dynamic correlation contribution, $\Delta\mathrm{E}cc$, is found as the difference between energies obtained using the MP2 and CCSD(T) methods, using the same cc-pV*n*Z-DK3 basis set. This basis set was used with *n*=T (triple-ζ) in composite method one, referred to as CM1, and with *n*=Q (quadruple-ζ) in composite method two (CM2). The dynamic correlation term was therefore calculated as

$$E_{CC} = E(CCSD(T)/cc-pVnZ-DK3, n=T,Q) - E(MP2/cc-pVnZ-DK3, n=T,Q) \qquad (9)$$

Both the MP2 and CCSD(T) energies in equation (6) utilized an active space with only the valence electrons included. For the actinide series of elements this includes any electrons in the 6*s*, 6*p*, 5*f*, 7*s* and 6*d* orbitals. The contribution for core-core and core-valence interactions, $\Delta\mathrm{E}cv$, was found as follows:

$$\Delta Ecv = E(CCSD(T)/sub-valence) - E(CCSD(T)/valence) \qquad (10)$$

The core-valence term is the difference between the CCSD(T) energy with a smaller frozen core, with both valence and sub-valence (5*s*, 5*d* and 5*p*) electron interactions treated in the active space, and the CCSD(T) energy with a larger frozen core (with only valence electrons included in the active space). In CM1, both the CCSD(T)/sub-valence and CCSD(T)/valence energies were found using the cc-pwCV*n*Z-DK3 basis set with *n*=D (double-ζ level) basis set. In CM2, the CCSD(T)/sub-valence and CCSD(T)/valence energy used *n*=T (triple-ζ level) basis set. All energies obtained for use in the first three terms in equation (6) (E_{ref}, ΔEcc and ΔEcv) utilized the third-order, spin-free Douglas-Kroll-Hess (DKH) Hamiltonian[79], and thus account only for scalar relativistic effects.

Finally, the last term in equation (6) is the previously introduced term accounting for spin-dependent (vector) relativistic effects in the Dirac Hamiltonian for the electronic energy (equation (3)). All of the scalar relativistic components for both the CCSD(T)+DHF composite method and α-ccCA (MP2 and CCSD(T) energies) were obtained using the MOLPRO2010 *ab initio* software package[94]. The spin-dependent DHF calculations were done using the DIRAC19 program[95].

Results and Discussion

I. General Considerations

Some of the early actinides, namely actinium (Ac) and protactinium (Pa), required correlation of the 7*s* spinors as well as the 6*d* spinors in the DHF calculations to obtain ionization potentials consistent with experiment. This was previously noted in work done by Feng and Peterson[61]. For actinium, CCSD(T) calculations were done in addition to the AOC-DHF calculation in order to calculate ΔE_{spin}. As this improved the accuracy of the first ionization energy for actinium, the CCSD(T) level ΔE_{spin} was used for the first ionization energy, which is shown in Table 1. As demonstrated in previous studies [76,96], relativistic effects (ΔE_{spin}) were found to be much larger between states where the *f*-orbital occupations change. For example, the second ionization energy for americium (between states with configurations of $5f^7 7s^1$ and $5f^7$) has a contribution (ΔE_{spin}) equal to 0.96 kcal mol^{-1}. In comparison, the contribution (ΔE_{spin}) to the second ionization energy for curium (between configuration states of $5f^7 7s^2$ and $5f^8$) is -7.5 kcal mol^{-1}. Even larger spin orbit contributions occur for most of the third ionization energies,and these tend to become larger across the series. Table 1 provides the electron configurations and electronic states considered in this work.

Table 1. Electronic states and configurations considered for the actinide (An) elements.

	An		**An$^+$**		**An^{2+}**		**An^{3+}**	
Ac	$6d^17s^2$	$^2D_{3/2}$	$7s^2$	$^1S_0$	$7s^1$	$^2S_{1/2}$	$6p^6$	$^1S_0$
Th	$6d^27s^2$	$^3F_2$	$6d^17s^2$	$^2D_{3/2}$	$5f^16d^1$	$^3H_4$	$5f^1$	$^2F_{5/2}$
Pa	$5f^26d^17s^2$	$^4K_{11/2}$	$5f^27s^2$	$^3H_4$	$5f^26d^1$	$^4I_{11/2}$	$5f^2$	$^3H_4$
U	$5f^36d^17s^2$	$^5L_6$	$5f^37s^2$	$^4I_{9/2}$	$5f^4$	$^5I_4$	$5f^3$	$^4I_{9/2}$
Np	$5f^46d^17s^2$	$^6L_{11/2}$	$5f^46d^17s^1$	$^7L_5$	$5f^5$	$^6H_{5/2}$	$5f^4$	$^5I_4$
Pu	$5f^67s^2$	$^7F_0$	$5f^67s^1$	$^8F_{1/2}$	$5f^6$	$^7F_0$	$5f^5$	$^6H_{5/2}$
Am	$5f^77s^2$	$^8S_{7/2}$	$5f^77s^1$	$^9S_4$	$5f^7$	$^8S_{7/2}$	$5f^6$	$^7F_0$
Cm	$5f^76d^17s^2$	$^9D_2$	$5f^77s^2$	$^8S_{7/2}$	$5f^8$	$^7F_6$	$5f^7$	$^8S_{7/2}$
Bk	$5f^97s^2$	$^6H_{15/2}$	$5f^97s^1$	$^7H_8$	$5f^9$	$^6H_{15/2}$	$5f^8$	$^7F_6$
Cf	$5f^{10}7s^2$	$^5I_8$	$5f^{10}7s^1$	$^6I_{17/2}$	$5f^{10}$	$^5I_8$	$5f^9$	$^6H_{15/2}$
Es	$5f^{11}7s^2$	$^4I_{15/2}$	$5f^{11}7s^1$	$^5I_8$	$5f^{11}$	$^4I_{15/2}$	$5f^{10}$	$^5I_8$
Fm	$5f^{12}7s^2$	$^3H_6$	$5f^{12}7s^1$	$^4H_{13/2}$	$5f^{12}$	$^3H_6$	$5f^{11}$	$^4I_{15/2}$
Md	$5f^{13}7s^2$	$^2F_{7/2}$	$5f^{13}7s^1$	$^3F_4$	$5f^{13}$	$^2F_{7/2}$	$5f^{12}$	$^3H_6$
No	$5f^{14}7s^2$	$^1S_0$	$5f^{14}7s^1$	$^2S_{1/2}$	$5f^{14}$	$^1S_0$	$5f^{13}$	$^2F_{7/2}$
Lr	$5f^{14}7s^27p^1$	$^2P_{1/2}$	$5f^{14}7s^2$	$^1S_0$	$5f^{14}7s^1$	$^2S_{1/2}$	$5f^{14}$	$^1S_0$

II. CCSD(T)+DHF

The ionization energies determined using the CCSD(T)+DHF approach are shown in Tables 2 (first ionization energies), 3 (second ionization energies) and 4 (third ionization energies). Experimental and previous theoretically determined ionization potentials are given for comparison.

Comparison to experimental data and previous theoretical work

As noted earlier, one of the most challenging aspects of theoretical work on the actinide series is the limited amount of experimental data to which to compare. However, a benefit of focusing on ionization energies is that there is some data available. Experimental results used for comparison to the ionization energies from this work are collected from the NIST database[97] and are shown in Table 2. The first ionization energy for actinium (24.0709 ± 0.0006 kcal mol^{-1}) was experimentally determined using Resonance Ion Spectroscopy (RIS) where three different Rydberg series [98] were analyzed. This work is in good agreement (<0.01 kcal mol^{-1} difference) with an earlier experimental result obtained by Resonance Ionization Mass Spectrometry (RIMS) [99]. Both RIS and RIMS are highly sensitive spectroscopic methods that are effective in the measurement of ionization potentials of radioactive samples that are often available only in trace amounts.

The first ionization energies for thorium (Th), neptunium (Np), plutonium (Pu), americium (Am), curium (Cm), berkelium (Bk) and californium (Cf) were determined using RIMS by Köhler and coworkers [100]. Their work made use of a saddle-point model by extrapolating observed photoionization thresholds obtained at differing field strengths to zero field strength. Samples of 10^{12} atoms were used, and the first ionization potentials for americium, curium, berkelium, and californium were measured for the first time. The "experimental" ionization potentials given in Table 2 for protactinium (Pa), fermium (Fm), and mendelevium (Md) are semi-empirical estimates. The energy levels needed to determine the first ionization energy have not been determined experimentally, but rather were extrapolated from experimentally known energy levels using the Rydberg-Ritz formula by Sugar [101]. In that study, the ionization energy was derived. The *ab initio* ionization potentials determined in this work at the quadruple-ζ level are consistent with reference [101], with a difference of ~1 kcal mol^{-1}.

As the first actinide element discovered, uranium is the most widely experimentally characterized element of the actinide series. The empirical ionization potential given in Table 2 was obtained by Coste and coworkers [102], The experimental value for einsteinium (Es) in Table 2 was determined again using RIMS by Waldek and coworkers[99]. Nobelium's first ionization potential was recently determined with high precision (to within 0.001 kcal mol^{-1}) using laser spectroscopy by Chhetri and coworkers[103]. Finally, the experimental first ionization energy for lawrencium (Lr) in Table 2 was determined by Sato and coworkers through surface-ion experiments[104]. The current work overestimates the first ionization potential for uranium; previous theoretical work [61] *underestimated* this value by about the same amount (~4-5 kcal mol^{-1}).

Figure S1 in the Supplementary Information (SI) provides the root-mean-square deviation (RMSD) in kcal mol^{-1} from experiment for the first ionization energies for all elements in the actinide series determined with the CCSD(T)+DHF composite. The calculated ionization energies for all data sets considered (VNZ, WNZ-V, WNZ-S, and CBS) in the current work, regardless of basis set and electron correlation approach, result in an RMSD of < 1 kcal mol^{-1}. For comparison, the energies from Feng and Peterson [61] that were obtained using the FPD Composite Approach based on energies obtained using MRCI+Q were found using frozen core (1*s*-5*d*) CBS-extrapolated values, and the eXact 2-component (X2C) cc-pwCVnZ-X2C (n = T, Q) basis sets optimized for outer-core correlation. These energies result in an RMSD of 5.59 kcal mol^{-1}. Cao and Dolg [76] used relativistic PP calculations at the CASSCF and MRACPF level of theory, corrected for spin-orbit interaction and PP errors. As

mentioned previously, Gaussian basis sets were used in the Cao and Dolg study [76]. These energies resulted in a RMSD of 6.67 kcal mol^{-1}. Thus, the CCSD(T)+DHF calculations offer a significant improvement in accuracy, overall, as compared with previous theoretical work; the WQZ-S set, which utilized the cc-pwCVQZ-DK3 basis set with valence and outer-core electron correlation, has the smallest RMSD for a single basis set, at just 0.46 kcal mol^{-1}. The CBS extrapolation of the cc-pwCVnZ-DK3 basis sets with valence and outer-core electrons active results in a RMSD for the first ionization energies of 0.38 kcal mol^{-1}.

Figure 1 shows the first ionization energies determined with CCDS(T)+DHF extrapolated to the CBS limit with valence and outer-core electrons in the correlation space in comparison to prior theoretical work and to experiment.

The empirical data for the second ionization potentials of the actinide series (Table 3) is limited, and only available for actinium, thorium, and uranium. The experimental value for actinium (271.05 ± 0.69 kcal mol^{-1}) was determined in the same manner (using the Rydberg-Ritz formula and extrapolation from experimentally determined energy levels) as the first ionization potentials for protactinium, fermium, and mendelevium [105]. The second ionization energy determined for Ac using the CCSD(T)+DHF composite extrapolated to the CBS limit is 0.10 kcal mol^{-1} below the range of empirical error, at 270.26 kcal mol^{-1}. This value, using only a coupled cluster-based approach, is only 0.19 kcal mol^{-1} below the MRCI+Q value obtained by Feng[61].

Table 3: Second ionization energies for the actinide series of elements, using different basis sets and electron correlation in kcal mol^{-1}. Here, VNZ=cc-pVnZ-DK3 basis set with valence correlation, WNZ-V=cc-pwCVnZ-DK3 with valence correlation, WNZ-S=cc-pwCVnZ-DK3 basis set with valence and outer-core correlation, and CBS=cc-pwCVnZ-DK3 with valence and outer-core correlation, extrapolated to the CBS limit.

	Ac[i]	Th	Pa	U	Np	Pu	Am	Cm	Bk	Cf	Es	Fm	Md	No	Lr
VDZ	267.49	289.48	268.02	271.74	267.19	265.48	270.21	296.89	277.14	280.18	283.30	286.75	289.63	292.18	330.88
VTZ	268.64	289.84	270.17	272.20	265.94	268.11	273.01	292.92	279.94	283.36	286.45	289.87	292.81	295.39	333.41
VQZ	268.85	288.65	269.70	270.94	265.31	268.75	273.70	289.59	280.69	284.20	287.34	290.79	293.74	296.46	334.43
WDZ-V	267.85	289.93	276.97	272.78	267.80	265.81	270.55	297.68	276.16	280.59	283.65	285.32	289.99	292.55	331.23
WTZ-V	268.61	289.58	270.22	272.19	265.78	268.25	273.18	292.12	280.12	283.57	286.71	290.15	293.08	295.68	333.76
WQZ-V	268.81	289.31	269.71	270.95	265.22	268.76	273.73	289.37	279.56	284.27	287.42	289.01	293.86	296.58	334.57
WDZ-S	268.93	295.38	271.56	277.01	269.60	267.01	271.74	301.59	276.72	281.69	284.58	285.48	290.76	293.32	331.81
WTZ-S	269.86	289.88	273.98	273.59	265.52	269.31	274.30	295.15	281.28	284.62	287.63	290.89	293.86	296.46	334.33
WQZ-S	270.12	286.53	271.64	270.62	263.34	269.67	274.71	291.49	279.89	285.22	288.28	289.09	294.59	297.34	335.13
CBS	270.3	286.7	272.1	270.6	263.1	270.0	275.1	291.3	280.1	285.6	288.7	288.3	295.0	297.7	335.3
Reference[ii]	270.5	281.0	273.2	276.4	267.3	266.0	270.9	284.7	275.1	278.0	281.2	284.1	287.1	290.1	334.6
Reference[iii]	267.5	280.2	274	274.9	267	265	269	286	276	278	281	285	287	290	335.3
Experimental[iv]	271.1	279	-	268	-	-	-	-	-	-	-	-	-	-	-

[i] Actinium values use the CCSD(T) method for the spin-orbit correction

[ii] FPD composite approach/MRCI Ref [61], truncated after the first decimal place in this table

[iii] Theoretical values obtained from the NIST Database[97],from Cao and Dolg [76]

[iv] Experimental data are taken from the NIST Database[97] and truncated after the first decimal place in this table when relevant

Table 4: Third ionization energies for the actinide series of elements, using different basis sets and electron correlation in kcal mol^{-1}. Here, VNZ=cc-pVnZ-DK3 basis set with valence correlation, WNZ-V=cc-pwCVnZ-DK3 with valence correlation, WNZ-S=cc-pwCVnZ-DK3 basis set with valence and outer-core correlation, and CBS=cc-pwCVnZ-DK3 with valence and outer-core correlation, extrapolated to the CBS limit.

	Ac[i]	Th	Pa	U	Np	Pu	Am	Cm	Bk	Cf	Es	Fm	Md	No	Lr
VDZ	397.38	413.56	429.72	437.68	458.30	480.73	499.30	453.82	489.13	511.99	525.68	538.83	550.54	605.25	496.31
VTZ	400.24	416.51	433.80	444.45	458.97	488.15	506.84	466.01	500.32	522.47	538.24	553.10	563.72	617.31	499.82
VQZ	400.53	417.59	434.64	447.01	461.92	490.99	509.80	471.17	505.12	526.97	543.38	558.66	569.15	622.69	501.26
WDZ-V	397.92	413.72	429.72	437.50	450.28	480.32	498.83	454.06	488.67	511.72	525.74	538.99	550.46	605.01	496.82
WTZ-V	400.26	416.43	432.74	444.73	459.47	488.58	507.37	467.32	502.21	523.50	539.69	554.72	565.34	619.04	500.41
WQZ-V	400.49	417.65	434.43	447.01	462.01	491.02	509.83	471.53	505.41	527.29	543.70	559.02	569.43	622.99	501.47
WDZ-S	399.80	412.81	430.84	436.81	450.84	478.66	495.20	452.22	485.97	506.49	521.97	535.58	546.03	598.15	497.63
WTZ-S	402.52	414.95	431.60	446.23	461.40	488.29	504.44	466.33	499.64	519.28	536.26	551.19	560.92	612.00	501.24
WQZ-S	402.85	416.50	434.58	450.08	465.32	492.01	508.17	471.36	504.46	523.91	540.99	556.12	565.62	616.59	502.29
CBS	403.2	417.1	435.8	450.8	466.2	492.9	508.9	472.3	503.7	525.0	542.4	557.7	567.2	618.0	502.7
Reference[ii]	402.2	421.6	426.5	435.4	455.8	488.4	508.7	467.3	503.5	530.5	537.3	549.1	577.7	611.9	501.0
Reference[iii]	403.8[iv]	419.9	430[vi]	433.5	453	485	502	464	497	519	523	533	560	594	502.7
Experimental[v]	-	422.5	-	457	-	-	-	-	-	-	-	-	-	-	-

[i] Actinium values use the CCSD(T) method for the spin-orbit correction

[ii] FPD composite approach/MRCI Ref [61], truncated after the first decimal place in this table

[iii] Theoretical values obtained from the NIST Database[97], from Cao and Dolg [76] unless otherwise noted

[iv] DC-CCSD(T)+Breit [114]

[v] Experimental data are taken from the NIST Database [97]

[vi] PP-CASSCF/MRACPF/CBS[115]

The second ionization energy of thorium (Th) was determined in prior work using ionization trap two-step laser excitation[106]. The CBS extrapolated CCSD(T)+DHF composite results in a second ionization energy of thorium of 286.7 kcal mol^{-1}, lying above the experimental value of 279.0 ± 4.6 kcal mol^{-1}. In the ionization trap two-step laser excitation work [106], 43 energy levels were observed for the Th^+ ion, within a 1 eV (~23 kcal mol^{-1}) energy range. Additionally, thorium exhibits strong coupling and near degeneracy between nuclear and electronic motions, apparent in the hyperfine structure. The multi-reference character for the Th^+ ion was also noted in an experimental spectroscopic and theoretical quantum chemical study done on ThO^+ and ThC^{+}[107]. This multi-reference nature may result in the overestimation of the ionization potential by single-reference methods such as CCSD(T).

In addition to the second ionization energy reference data in Table 3 provided from FPD/MRCI+Q[61], previous values obtained using PP-CASSCF/MRACPF are again given for comparison [76]. Figure S2 in the SI shows the CCSD(T)+DHF CBS data for the second ionization energy in comparison to prior work. The experimental second ionization energy for uranium (268 ± 9 kcal mol^{-1}) was determined by Blaise and coworkers [108]; the poor reliability of this result has been discussed previously[109]. The second ionization energy obtained using the FPD composite based upon MRCI+Q energies [61] is reported as 276.42 kcal mol^{-1}; the PP-CASSCF/MRACPF second ionization energy [76] for uranium is given as 274.9 kcal mol^{-1}. The value of 276.42 kcal mol^{-1} is reported in Table 3, as it was determined in the same manner and in the same work by Feng and Peterson[61] as the rest of the ionization potentials used for comparison here. However, it should be noted that in earlier work by Peterson and coworkers on the first six IP's for the uranium atom, the second ionization potential for uranium was determined to be 271.2 kcal mol^{-1} [109], in much better agreement with experiment than the ionization potential (276.42 kcal mol^{-1}) determined in [61] . This value was also determined using the FPD composite and MRCI+Q energies; the difference in the two values is thus attributed to the contraction scheme used in the MRCI+Q treatment, as well as the methods used for obtaining the spin-orbit correction[61]. Specifically, the spin-orbit correction in [109] was carried out with the Kramers-restricted configuration interaction (KRCI)[110–112] method, whereas the treatment for the spin-orbit correction in [61] utilized the AOC- DHF level of theory. The CCSD(T)+DHF composite value (270.6 kcal mol^{-1}) deviates less than 0.6 kcal mol^{-1} from the FPD /MRCI+Q result in [109].

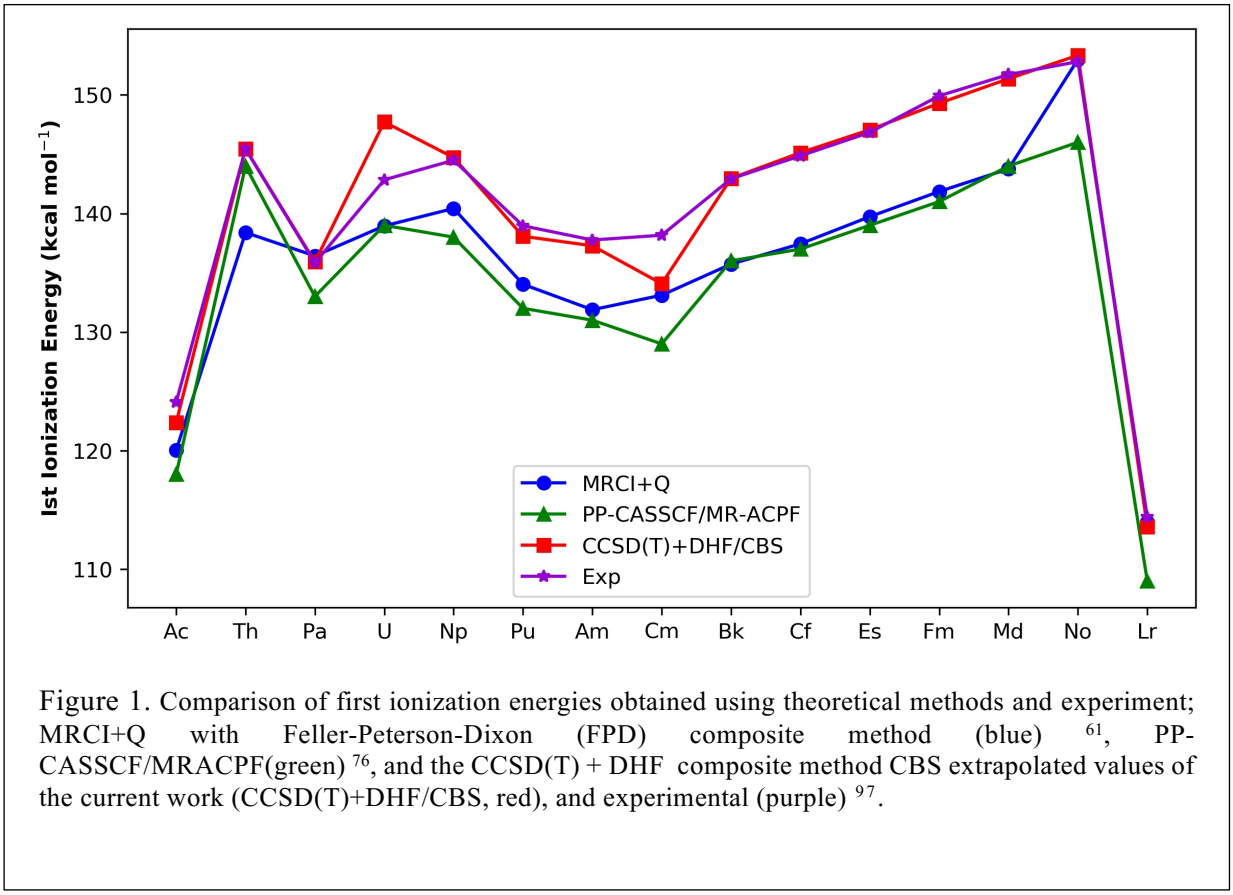

Figure 1. Comparison of first ionization energies obtained using theoretical methods and experiment; MRCI+Q with Feller-Peterson-Dixon (FPD) composite method (blue) [61], PP-CASSCF/MRACPF(green) [76], and the CCSD(T) + DHF composite method CBS extrapolated values of the current work (CCSD(T)+DHF/CBS, red), and experimental (purple) [97].

Only two elements have available experimental third ionization energies in the NIST database (see Table 4): thorium [113] and uranium [108]. The experimental value for the third ionization energy for thorium is semi-empirical and has a value of 422.5 ± 1.2 kcal mol^{-1}. The current study underestimates this value, with an ionization energy of 417.1 kcal mol^{-1} obtained using the CCSD(T)+DHF method. The CCSD(T)+DHF method performs much better for the uranium third ionization energy: the experimental value is 457 ± 7 kcal mol^{-1}; the CCSD(T)+DHF with CBS extrapolation results in 450.8 kcal mol^{-1}, within the experimental error range . This value is in much better agreement with experiment than the previously obtained theoretical values. The performance of the CCSD(T)+DHF method in comparison to the experimental values offers some interesting insight. As discussed previously, thorium is known to possess strong multireference character. However, the electron configurations of the Th^{2+} and Th^{3+} ions are $5f^1 6d^1$ and $5f^1$, respectively. The electron configurations of the U^{2+} and U^{3+} ions are $5f^4$ and $5f^3$, respectively. While spin-orbit effects are known to be large for ionization potentials between two ions that contain different *f*-orbital electron occupations (such as is the case for uranium), it can be inferred that there are even larger effects that are not being accounted for when considering ionization potentials between two ions of different total angular momenta (such as is the case for thorium). See Figure S3 in the SI for a comparison of the performance of theoretical methods when determining the third ionization energy.

Effect of basis set and electron correlation space choice for CCSD(T)+DHF

For the first ionization energies (Table 2), the additional electron correlation included in the active space for WNZ-S as compared to WNZ-V does improve the accuracy of the energy values compared to experiment for most elements. This is clear from the RMSD from experimental values as discussed previously. The difference in energies between WNZ-V and WNZ-S is quite small for most elements (less than 1 kcal mol^{-1}, or far less than 1 percent of the total ionization energy). However, energies obtained using basis sets of different cardinal numbers (n=D,T,Q) display an increase in precision when outer-core electrons are included in the active/correlation space, versus energies obtained using only valence electrons in the active space. For example, the standard deviation between the double-ζ, triple-ζ and quadruple-ζ values for protactinium (Pa) when valence electrons are correlated only is 2.25 kcal mol^{-1}, while the standard deviation between the same basis sets obtained when both valence and outer-core correlation is included in the active space is 1.71 kcal mol^{-1}.

In Table 3, the effect of electron correlation on the second ionization energies is shown. There is a significantly larger difference between the WNZ-V and WNZ-S data sets when considering the second ionization energies than when comparing values for the first ionization energies. The differences tend to decrease at the quadruple-ζ level. Including sub- valence electron correlation in the active space is important for obtaining accurate values of the second ionization energies when compared to experiment. For example, the second ionization energy for thorium is 289.31 kcal mol^{-1} (WQZ-V) and the value obtained using outer-core correlation (WQZ-S) is 286.53 kcal mol^{-1}. Additional correlated electrons thus bring the second ionization energy value ~3 kcal mol^{-1} closer to the experimental value.The same is true for the second ionization energies obtained for actinium and uranium; outer-core correlation significantly increases the accuracy of these energies with respect to experimental data.

The third ionization potentials (Table 4) obtained in the WNZ-V and WNZ-S data sets display larger differences than those observed between the two sets for the second ionization energies. For most elements this difference again decreases with increasing cardinal number (n); for example, there is a smaller difference between the WQZ-V and WQZ-S set than between the WTZ-V and WTZ-S data set. For the third ionization energies, using sub-valence electron correlation is indispensable for obtaining accurate values when compared to experimental data. For uranium for example, the ionization energy obtained at the WQZ-V level is 447.01 kcal mol^{-1}, while the ionization energy obtained at the WQZ-S level is 450.08 kcal mol^{-1}, or more than 3 kcal mol^{-1} closer to experiment.

The cc-pVDZ-DK3 and cc-pwCVDZ-DK3 basis sets generally underestimate the first ionization potentials by as much as 5-6 kcal mol^{-1}. This error is apparent in the RMSD discussed previously and shown in Figure S1 in the SI. The RMSD for the first ionization energy falls quite dramatically (from ~0.90 kcal mol^{-1} to ~0.57 kcal mol^{-1}) when the cardinal number is increased to the triple-ζ level (n=T) regardless of which basis set is used (cc-pV*n*Z-DK3 or cc-pwCV*n*Z-DK3). For the second ionization potentials, the difference between the data obtained at the double-ζ basis set level versus that obtained with the triple- or quadruple-ζ basis set is not as large as the differences for the first ionization energies. For example, the cc-pwCVDZ-DK3 (WDZ-V) second ionization energy is 267.9 kcal mol^{-1}, while the second ionization energy obtained using the cc-pwCVQZ-DK3 (WQZ-V) basis set is only about 1 kcal mol^{-1} larger, at 268.8 kcal mol^{-1}. Therefore, this property is not as

sensitive to the size of the basis set. However, the most accurate energies obtained utilized the quadruple-ζ level basis sets. Examining the third ionization potentials for basis set dependence shows that they are most sensitive to size of basis set used. For many elements, the difference between the third ionization energy obtained at the double-ζ and quadruple-ζ levels is 10 kcal mol^{-1} or larger, and for some of the later actinides this difference even surpasses 20 kcal mol^{-1} (see Figure 2 for a basis set comparison of all third ionization energies obtained in this work). The differences between the triple-ζ and quadruple-ζ basis sets are generally much smaller, not more than 4-5 kcal mol^{-1}. Therefore, using a basis set of at least triple-ζ quality is essential for calculation of the third ionization energies. As the actinides often form An(III) cations during thermodynamic processes, it is important to use at least a triple-ζ level basis set when obtaining thermodynamic properties using the CCSD(T)+DHF composite method as well. In considering the impact on the accuracy of the ionization energies of choosing the cc-pwCVnZ-DK3 or cc-pVnZ-DK3 basis sets, there is not much of a difference for the first, second, or third ionization energies. For most elements in fact, the difference is far below 1 kcal mol^{-1}.

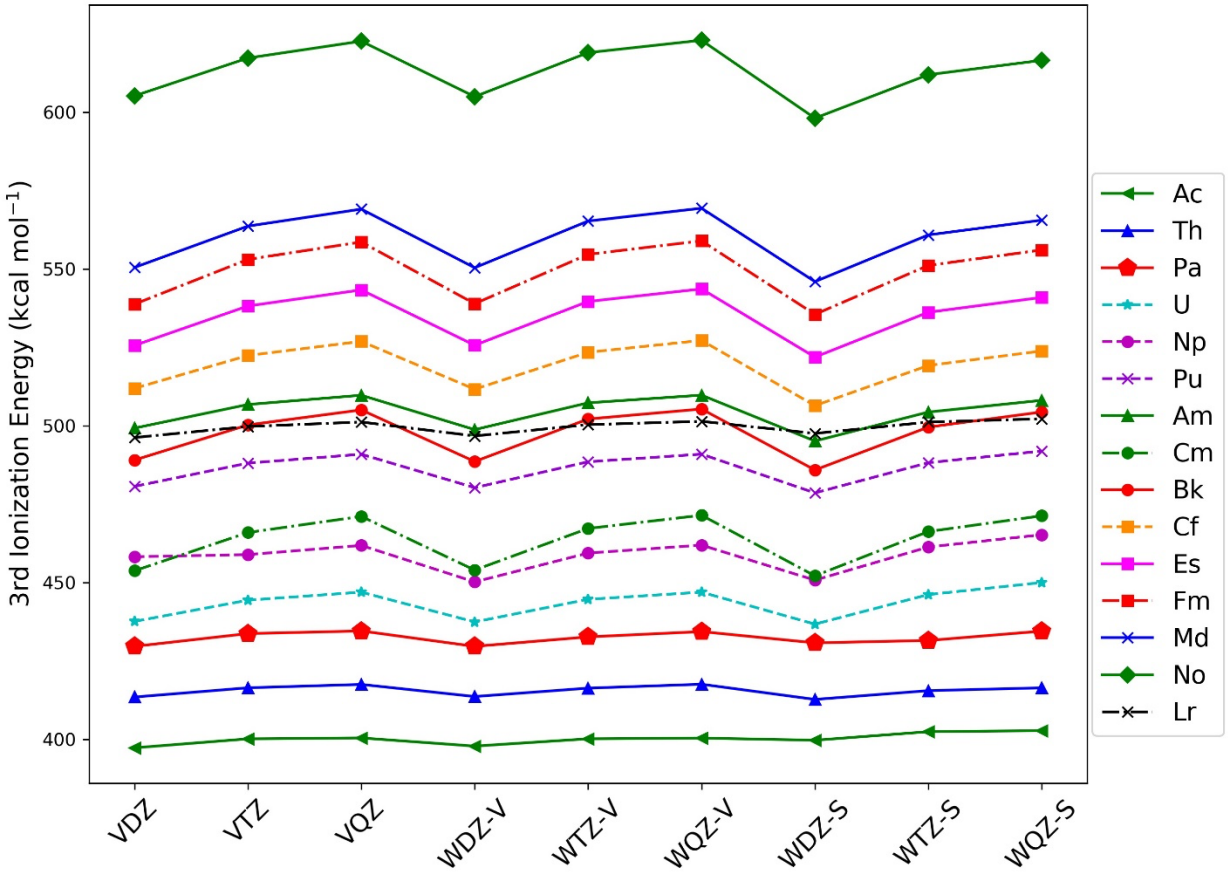

Figure 2. Third ionization energies obtained with the CCSD(T)+DHF ,at all basis set and electron correlation levels considered, in kcal mol^{-1}.

III. Ionization potentials determined within α-ccCA formalism

To further reduce computational cost in comparison to the CCSD(T)+DHF/CBS extrapolated scheme, a ccCA formulism was used to obtain the first, second, and third ionization potentials for the entire series of actinide elements (as outlined in the methods section). Here, the performance of extrapolation schemes for the HF and MP2 energies is first examined, followed by an assessment of the method in terms of accuracy and cost relative to the CCSD(T)+DHF method.

Performance of Extrapolation Schemes

As mentioned in the computational methods section, the HF and MP2 energies were extrapolated separately to the CBS limit. To investigate the impact of different extrapolation schemes on the accuracy of the ionization potentials with respect to experimental data, nine different combinations of extrapolation schemes using equations (4)[85,88], (5)[89,90], (7)[92] and (8)[93] were employed, with both two- and three-point extrapolations considered. The two-point extrapolations utilized *n*=T,Q or triple- and quadruple-ζ level energies. The three-point extrapolations additionally included *n*=D (double-ζ) level energies. For simplicity, these nine extrapolation combinations are labeled A-I and correspond to the combinations given in Table 5. Equation (7) was attempted using a two-point extrapolation as well as a three-point extrapolation but using just the triple- and quadruple-ζ HF energies in this formula gave an extremely poor fit to the data, with R^2 values well below 0.1, and thus this data was excluded.

Table 5. For simplicity, labels are provided to identify combinations of extrapolation formulas used to obtain the CBS limit for HF and MP2 energies, using the cc-pVnZ-DK3 basis set and valence electron correlation. All of the formulas are in the form $E_n = E_\infty + X$, where X is shown in the table. The labels are subsequently used in Figure 8.

Label	HF Formula, X=	n=	MP2 Formula, X=	n=
A	$Ae^{(-1.63n)}$	T,Q	$A(n+0.5)^{-4}$	D,T,Q
B	$Ae^{(-1.63n)}$	D,T,Q	$e^{(-(n-1))} + Be^{(-(n-1)^2)}$	D,T,Q
C	$A(n+1)e^{(-6.57\sqrt{n})}$	D,T,Q	$e^{(-(n-1))} + Be^{(-(n-1)^2)}$	D,T,Q
D	$Ae^{(-1.63n)}$	D,T,Q	$A(n+0.5)^{-4}$	D,T,Q
E	$Ae^{(-1.63n)}$	T,Q	$A(n+0.5)^{-4}$	T,Q
F	$A(n+1)e^{(-6.57\sqrt{n})}$	D,T,Q	$A(n+0.5)^{-4}$	D,T,Q
G	$A(n+1)e^{(-6.57\sqrt{n})}$	D,T,Q	$A(n+0.5)^{-4}$	T,Q
H	$Ae^{(-1.63n)}$	T,Q	$Ae^{(-(n-1))} + Be^{(-(n-1)^2)}$	D,T,Q
I	$Ae^{(-1.63n)}$	D,T,Q	$A(n+0.5)^{-4}$	T,Q

The total first ionization energies determined with α-ccCA resulting from these extrapolations of the reference energy were then compared to experimental first ionization energies available from NIST[97] (see Table 2). To determine which extrapolation scheme A-I gave the best result, the root-mean-square deviation (RMSD) from experimental data was found for the first ionization energies using each combination of extrapolation formulas, for both CM1 and CM2 (described in the methods section). The RMSD is shown in Figure 3. From the RMSD, composite scheme A performs the best overall, with a RMSD of 1.84 kcal mol^{-1} for CM1 and 1.89 kcal mol^{-1} for CM2. The second and third lowest RMSD occurs for composite schemes D (CM1:1.91 kcal mol^{-1}, CM2:2.02 kcal mol^{-1}) and F (CM1: 1.91 kcal mol^{-1}, CM2:2.03 kcal mol^{-}

[1]). This offers the following insights: equation (4) is a better choice than the Karton-Martin formula (equation (5)) for finding the CBS limit of the HF energies for the actinide series of elements overall. Additionally, a two-point extrapolation of equation (4) performs better than the same formula using a three-point extrapolation. In other words, the use of the energies obtained using the cc-pVDZ-DK3 basis set are not favorable for obtaining the most accurate first ionization energies with respect to experimental data. This indicates that when calculating HF energies for the actinide elements, basis sets containing [*spdfgh*] functions at a minimum are important.

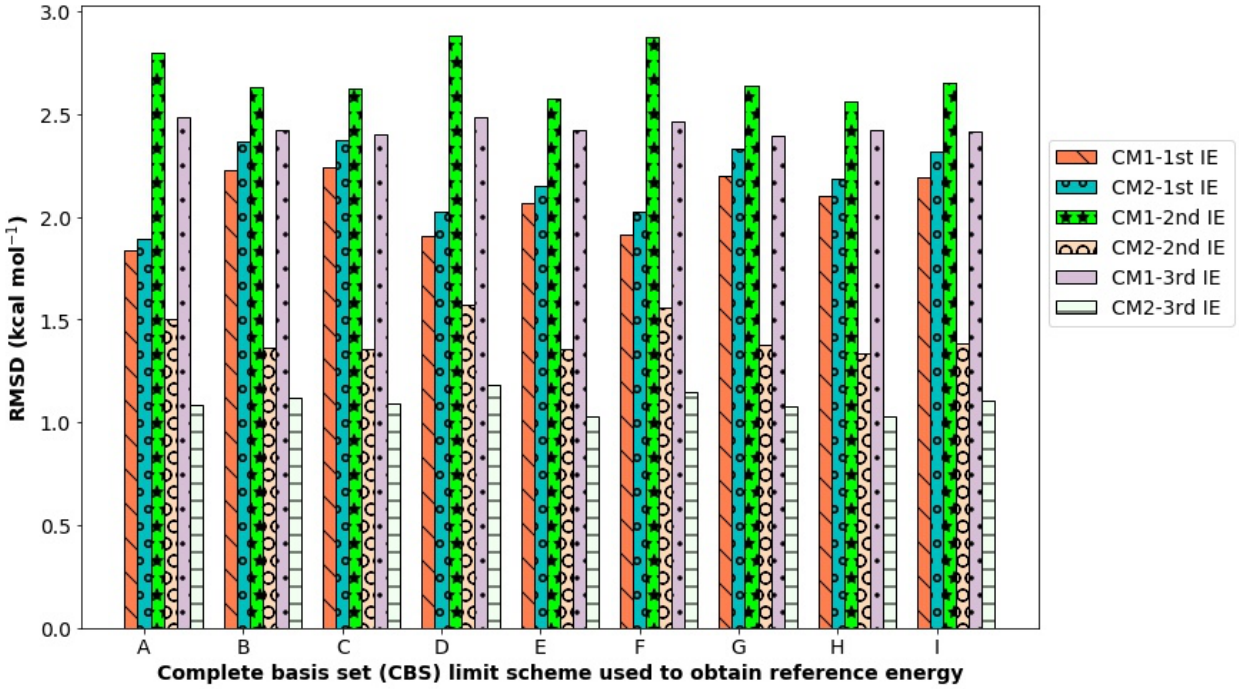

Figure 3. Root-mean-square deviation (RMSD) of the first ionization energies from experiment for the CM1 and CM2 approach for each of the CBS routes (A-I) to the reference energy in the composite. For the second and third ionization energies, the RMSD is relative to CCSD(T) + DHF/ CBS extrapolated energies.

For the MP2 correlation energy, the same RMSD data indicates that the use of equation (5), with a three-point extrapolation versus a two-point, provides the most accurate route to obtain the first ionization potentials overall, when added to the two-point extrapolated HF energies.

There is limited experimental data for comparison to the α-ccCA second ionization energies. Therefore the RMSD from the second ionization energies obtained using CCSD(T)+DHF method of section II, with valence and sub-valence electrons in the active space, and the cc-pwCVnZ-DK3 basis set extrapolated to the CBS limit is used for comparison. This RMSD from the CCSD(T)+DHF method for the second ionization energies for CM1 and CM2 using extrapolation schemes A-I for the reference energy is shown in Figure 3 as well. For the second IE's obtained using CM1, the nine extrapolation schemes give

RMSD's that are within a spread of ~0.32 kcal mol^{-1}. Regardless of extrapolation scheme used, the second ionization energies have an RMSD from the CCSD(T)+DHF/CBS second ionization energies of < 3 kcal mol^{-1}. For CM2, the spread between RMSD values for the second ionization energy extrapolation schemes is smaller, around 0.24 kcal mol^{-1}. The RMSD from the CCSD(T)+DHF/CBS second ionization energies when using CM2 is near or below 1.5 kcal mol^{-1}. Because there is not enough experimental data to compare the second ionization energies to, and extrapolation scheme A worked best for the first ionization energies with regard to experiment, scheme A will again be used for the second ionization energies. The very small spread in RMSD (less than 0.5 kcal mol^{-1}) as mentioned above, depending on if CM1 or CM2 is being used, helps validate this choice.

Because there is also limited experimental data available for the third ionization energies, the RMSD with respect to the CCSD(T)+DHF composite values is shown in Figure 3 also. The spread in RMSD values is ~ 0.1 kcal mol^{-1} for CM1, and 0.15 kcal mol^{-1} for CM2. For CM1, the RMSD from the third ionization energies determined using CCSD(T)+DHF/CBS is ~2.5 kcal mol^{-1}, regardless of extrapolation scheme used. . For CM2, the RMSD from the third ionization energies determined using CCSD(T)+DHF/CBS is ~1 kcal mol^{-1}, regardless of extrapolation scheme used. Again, given the very small spread between the RMSD, and the lack of experimental data for which to compare, scheme A is used for the third ionization energies.

Comparison of α-ccCA formalisms with prior theoretical work and experiment

In this section the ionization energies obtained using α-ccCA (both CM1 and CM2) are compared to experimental ionization energies. Additionally, the individual terms in equation (6) (the total energy obtained using α-ccCA) are further examined.

In Table 6, the MP2 first ionization energies (E_{ref}) obtained using extrapolation scheme A, and used in both CM1 and CM2 are shown. Also in Table 6, the components of equation (6) used to obtain the first ionization energies using CM1 and CM2, the total ionization energies obtained using CM1 and CM2 , the ionization energies obtained using the CCSD(T)+DHF method from section II (labeled CBS), and the experimental ionization energies obtained from NIST[97] are listed as well.

Table 6. Components of the α-ccCA used to obtain the first ionization energies, total calculated ionization energies obtained using CM1 and CM2, and experimental ionization energies from NIST[97], in kcal mol^{-1}.[i]

		CM1				CM2					
An	$\mathbf{E_{ref}}$	$\mathbf{\Delta E_{CC}}$	$\mathbf{\Delta E_{CV}}$	$\mathbf{\Delta E_{spin}}$	$\mathbf{E_{tot}}$	$\mathbf{\Delta E_{CC}}$	$\mathbf{\Delta E_{CV}}$	$\mathbf{\Delta E_{spin}}$	$\mathbf{E_{tot}}$	**CBS**	**Exp**[ii]
Ac	119.3	1.93	-1.11	3.72	123.93	1.93	-1.39	3.72	123.65	122.3	124.0709(6)
Th	148.7	-2.24	-0.67	0.98	146.86	-2.23	-0.64	0.98	146.89	145.5	145.436(7)
Pa	139.5	-1.07	-0.69	-2.35	135.46	-1.34	-1.63	-2.35	134.25	135.9	135.8(28)
U	143.3	2.29	-1.36	3.61	147.95	2.28	-1.51	3.61	147.80	147.7	142.838(1)
Np	143.0	0.98	0.88	0.30	145.27	0.61	0.76	0.30	144.78	144.7	144.486(7)
Pu	136.0	-0.43	0.55	2.36	138.59	-0.66	0.41	2.36	138.23	138.1	138.958(7)
Am	137.1	-0.80	0.51	0.85	137.73	-1.04	0.42	0.85	137.41	137.3	137.759(7)
Cm	129.9	1.25	-0.48	4.23	134.97	1.07	-0.65	4.23	134.62	134.1	138.165(7)
Bk	143.3	-1.68	0.53	1.10	143.38	-1.94	0.44	1.10	143.02	143.0	142.925(7)
Cf	146.0	-2.19	0.56	1.12	145.58	-2.45	0.50	1.12	145.25	145.1	144.859(7)
Es	148.3	-2.47	0.50	1.06	149.98	-2.77	0.48	1.06	149.95	147.1	146.840(7)
Fm	151.0	-2.79	0.51	1.10	149.74	-3.11	0.48	1.10	149.39	149.3	149.9(16)
Md	153.2	-3.11	0.48	1.20	151.83	-3.45	0.47	1.20	151.49	151.4	151.7(16)
No	155.4	-3.46	0.49	1.32	153.83	-3.83	0.49	1.32	153.46	153.3	153.4(16)
Lr	91.7	3.38	-0.03	18.58	113.73	3.20	0.02	18.58	113.59	113.6	114.4(18)

[i] For CM1, the ΔE_{CC} term utilized the cc-pvtz-DK3 basis set, while the ΔE_{CV} term used the cc-pwCVDZ-DK3 basis set. In CM2, the ΔE_{CC} term utilized the cc-pvqz-DK3 basis set, while the ΔE_{CV} term used the cc-pwCVTZ-DK3 basis set.

[ii] The error in the experimental ionization energies for the last digits is given in parentheses.

Figure 4 shows the absolute difference between the first ionization energies obtained using CM1, CM2, CCSD(T)+DHF/CBS, and experimental values. The difference between experimental first ionization energies and those obtained using MRCI+Q/FPD[61] are also included for reference. From Figure 4, it is apparent that both CM1 and CM2 are consistent with the CCSD(T)+DHF energies, with the ionization energy for einsteinium (Es) being the only exception. The source of this error for Es arises from the core-valence term, ΔE_{CV}. For CM1 and CM2, this term contributes 0.50 kcal mol^{-1} and 0.48 kcal mol^{-1}, respectively, to the total first ionization energy. This term is likely underestimated. For example, the MRCI+Q/FPD[61] method for obtaining the first ionization energy results in a core-valence CBS extrapolated contribution of -1.52 kcal mol^{-1}.

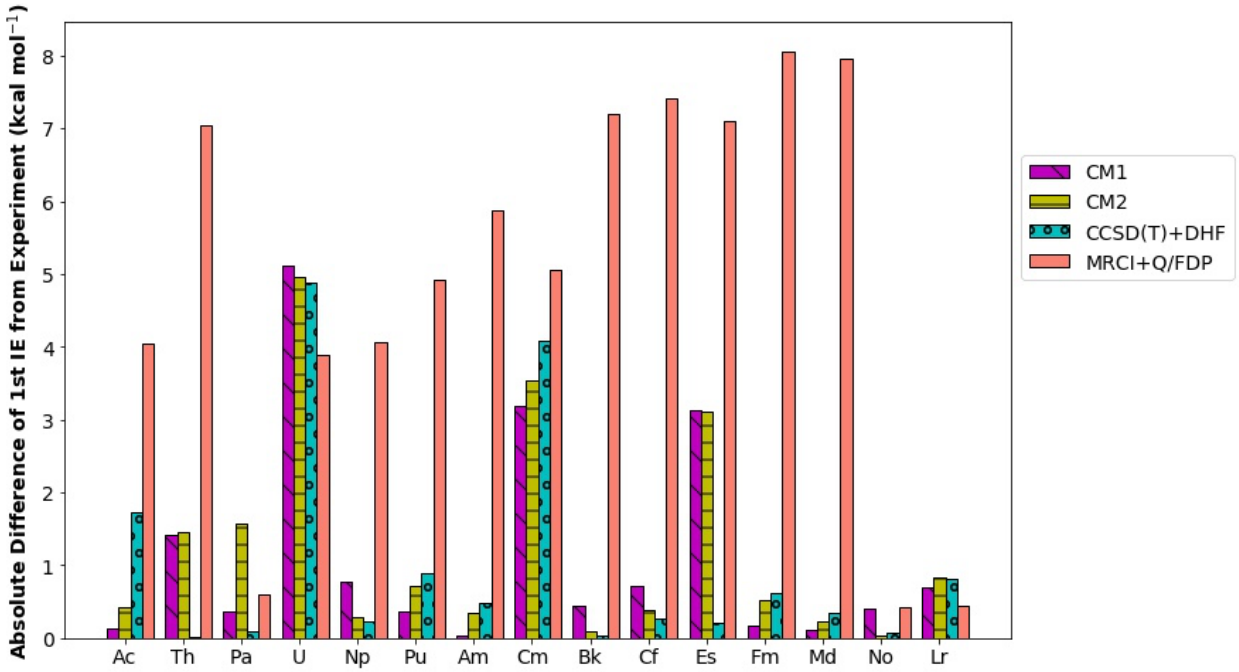

Figure 4. Absolute difference from experiment of first ionization energies obtained using CM1, CM2, the CCSD(T)+DHF/CBS composite method and MRCI+Q/FPD[61].

Table 7 gives the MP2 energy (E_{ref}) obtained using extrapolation scheme A, and used in both the CM1 and CM2 methods to obtain the second ionization energies. Also shown are the individual terms used in equation (1) to calculate the second ionization energies using CM1 and CM2, respectively, the total ionization energies obtained using CM1 and CM2, the ionization energies obtained with the CCSD(T)+DHF composite (labeled CBS), and the experimental values from NIST[97] where available.

Table 7. Components of the α-ccCA used to obtain the second ionization energies, total calculated ionization energies obtained using CM1 and CM2, and experimental ionization energies from NIST[97], in kcal mol^{-1}.[i]

		CM1				CM2					
An	$\mathbf{E_{ref}}$	$\mathbf{\Delta E_{CC}}$	$\mathbf{\Delta E_{CV}}$	$\mathbf{\Delta E_{spin}}$	$\mathbf{E_{tot}}$	$\mathbf{\Delta E_{CC}}$	$\mathbf{\Delta E_{CV}}$	$\mathbf{\Delta E_{spin}}$	$\mathbf{E_{tot}}$	**CBS**	**Exp**[ii]
Ac	267.9	1.61	1.08	-0.22	270.3	1.44	1.25	-0.22	270.3	270.3	271.05(69)
Th	290.4	3.36	5.45	-4.84	294.4	3.10	-0.37	-4.84	288.3	286.7	279.0(46)
Pa	272.2	2.54	1.55	-4.00	272.3	2.06	3.76	-4.00	274.1	274.1	-
U	264.2	2.40	4.22	4.70	275.5	2.19	1.40	4.70	272.5	270.6	268(9)
Np	250.7	4.58	1.80	9.35	266.4	4.79	-0.26	9.35	264.8	263.1	-
Pu	272.6	-4.97	1.21	-0.74	268.1	-2.65	1.06	-0.74	270.2	270.0	-
Am	276.5	-3.29	1.18	0.95	275.4	-3.33	1.12	0.95	275.3	275.1	-
Cm	291.7	4.91	3.91	-7.45	293.1	5.30	3.02	-7.45	292.6	291.3	-
Bk	284.2	-3.82	0.55	0.96	281.9	-3.95	1.16	0.96	282.4	280.1	-
Cf	288.4	-4.69	1.10	1.13	285.9	-4.79	1.05	1.13	285.8	285.6	-
Es	291.5	-4.91	0.94	1.42	289.0	-5.07	0.92	1.42	288.8	288.7	-
Fm	295.1	-5.23	0.16	1.63	291.7	-5.43	0.74	1.63	292.0	288.3	-
Md	298.3	-5.58	0.77	1.78	295.3	-5.82	0.77	1.78	295.1	295.0	-
No	301.5	-6.12	0.77	1.90	298.0	-6.37	0.79	1.90	297.8	297.7	-
Lr	338.7	-5.24	0.59	1.77	335.8	-5.70	0.57	1.77	335.4	335.3	-

[i] For CM1, the ΔE_{CC} term utilized the cc-pVTZ-DK3 basis set, while the ΔE_{CV} term used the cc-pwCVDZ-DK3 basis set . In CM2, the ΔE_{CC} term utilized the cc-pVQZ-DK3 basis set, while the ΔE_{CV} term used the cc-pwCVTZ-DK3 basis set .

[ii] The error in the experimental ionization energies for the last digits is given in parentheses.

The second ionization energies obtained using CM2 show a much smaller RMSD from those obtained using CCSD(T)+DHF, overall, than CM1, regardless of which HF/MP2 extrapolation is used (Figure 3). . The largest differences between CM1 and CM2 are seen near the beginning of the series, for elements Th, Pa U, Np, and Pu, and then again for Cm. Because of this, each of the individual term(s) in the composite are examined to determine what may be causing the differences. Because the reference energy and spin-orbit terms are identical for CM1 and CM2, this involves examination of ΔE_{CC} and ΔE_{CV}.

The values of ΔE_{CC} obtained using CM1 and CM2 are similar in terms of both sign and magnitude, differing by well under 0.5 kcal mol^{-1} for all elements except Pu. For Pu, this term is almost twice as large for CM1 as compared to CM2. This term is the source of the difference between the second ionization energy obtained using CM1 and CM2 for Pu.

The ΔE_{CV} term is responsible for the observed discrepancies between the second ionization energies for Th, Pa, U, Np and Cm obtained using CM1 and CM2. Considering the electron configurations for the states considered where there is a large difference in the ΔE_{CV} term for CM1 and CM2, it is shown that ionization does not occur in a simple electron removal process between these states. Rather, there is an additional rearrangement of the remaining valence electrons. For example, for $Th^{+} \rightarrow Th^{2+}$, an electron is not just removed from the doubly occupied *s*-orbital, leaving one electron remaining. Rather, this remaining electron is moved to an *f*-orbital. Similarly, for $Pa^{+} \rightarrow Pa^{2+}$, an electron does not remain in the *s*-orbital after one is removed, but rather now occupies a *d*-orbital. Similar rearrangements occur for U, Np, and Cm. The contribution of ΔE_{CV} to the second ionization energy of Th is positive, at 5.45 kcal mol^{-1}. The same term obtained using CM2 gives a negative contribution, at -0.37 kcal mol^{-1}. When using CM1, this term is the

difference between the energy obtained using the cc-pwCVDZ-DK3 basis set with valence and sub-valence electrons considered active, and the energy obtained using the same basis set but with only valence electrons active. For CM2, the term is obtained in the same way but using the cc-pwCVTZ-DK3 basis set. This indicates that for ionization energies that have significant core-core and core-valence interactions stemming from a rearrangement of electron configuration, using the double-ζ level basis set is not sufficient for recovery of this interaction. While the triple-ζ basis sets do better, this term is still lacking at this level to give an overall accurate ionization energy with respect to experimental values. For example, for Th, the core-core and core-valence CBS extrapolated correction term obtained using MRCI+Q/FPD[61] for the second ionization energy is larger than for any other element in the series, at -8.40 kcal mol^{-1}. Therefore, using CM2 this term at least has the correct sign. This large negative term would make up for the difference between the CM2 obtained second ionization energy for Th (288.3 kcal mol^{-1}) and the experimental value (279 kcal mol^{-1}). Even using the cc-pwCVQZ-DK3 basis sets and CCSD(T), this term is -2.78 kcal mol^{-1}; still much too small. Therefore, this is likely to be a consequence of using a single-reference method versus a multi-reference method.

The next large difference in the ΔE_{CV} term obtained using CM1 and CM2 occurs for the next element in the series, Pa. Unfortunately, there is not experimental data available for the second ionization energy for this element to compare to. The second ionization energy obtained using CM1 is 272.3 kcal mol^{-1}, with ΔE_{CV} = 1.55 kcal mol^{-1}. The second ionization energy obtained using CM2 is 274.1 kcal mol^{-1}, corresponding to ΔE_{CV} = 3.76 kcal mol^{-1}. Previous studies done at the MRCI+Q/FPD[61] and CASSCF/MR-ACPF-PP[76] levels of theory gave second ionization energies for Pa of 273.24 and 274 kcal mol^{-1}, respectively. Therefore, both CM1 and CM2 give a second ionization energy for Pa that is within 1 kcal mol^{-1} of that determined in these multi-reference studies, at a significantly reduced computational cost associated with a single reference method and a reduced number of basis functions.

There is a large difference in the ΔE_{CV} term obtained using CM1 and CM2 for calculation of the second ionization energy of U. This term contributes 4.22 kcal mol^{-1} when using CM1, and the calculated second ionization energy for this element is 275.5 kcal mol^{-1}. The ΔE_{CV} term obtained using CM2 is also positive, but only 1.40 kcal mol^{-1}, contributing to a second ionization energy of 272.5 kcal mol^{-1}; this value is 3 kcal mol^{-1} closer to the experimental second ionization energy for uranium, which is 268 ± 9 kcal mol^{-1}. Similarly, the core-core and core-valence correction terms for Np obtained using CM1 and CM2 are ~2 kcal mol^{-1} apart, and for Cm these terms are ~1 kcal mol^{-1} apart. The difference in the ΔE_{CV} term obtained using the two composite methods is not as pronounced for the remaining elements, often far under 0.5 kcal mol^{-1}.

Table 8 gives the MP2 CBS extrapolated energies (E_{ref}) obtained using extrapolation scheme A and used in both CM1 and CM2 to obtain the third ionization energies. Table 8 also gives the individual terms used in equation (6) to calculate the third ionization energies using CM1 and CM2, respectively, the total ionization energies using CM1 and CM2, the CCSD(T)+DHF composite total ionization energies, and the experimental values from NIST[97] where available.

Table 8. Components of α-ccCA used to obtain the third ionization energies, total calculated ionization energies obtained using CM1 and CM2, and experimental ionization energies from NIST[97], in kcal mol^{-1}. [i]

		CM1				CM2					
Element	E_{ref}	ΔE_{CC}	ΔE_{CV}	ΔE_{spin}	E_{tot}	ΔE_{CC}	ΔE_{CV}	ΔE_{spin}	E_{tot}	**CBS**	**Exp**[ii]
Ac	400.1	0.31	1.88	0.52	402.8	0.25	2.26	0.52	403.2	403.2	-
Th	408.2	3.24	-0.92	6.50	417.0	3.15	-0.80	6.50	417.1	417.1	422.5(12)
Pa	421.1	1.48	-5.80	11.42	428.2	2.02	-1.1	11.42	433.5	435.8	-
U	454.9	-3.81	-0.69	-3.57	446.8	-3.81	1.50	-3.57	449.0	450.8	456.6(69)
Np	477.6	-9.39	0.56	-4.93	463.8	-9.33	1.94	-4.93	465.2	466.2	-
Pu	505.8	-6.95	-1.66	-6.80	490.4	-7.14	-0.29	-6.80	491.6	492.9	-
Am	547.5	-9.34	-3.63	-27.36	507.1	-9.46	-2.94	-27.36	507.7	508.9	-
Cm	473.8	-10.51	-1.84	9.52	471.0	-11.21	-0.98	9.52	471.1	472.3	-
Bk	516.0	-13.30	-2.70	4.35	504.4	-13.83	-2.58	4.35	504.0	503.7	-
Cf	545.2	-12.52	-5.23	-3.39	524.0	-13.44	-4.21	-3.39	524.1	525.0	-
Es	577.2	-19.84	-3.77	-11.88	541.7	-20.44	-3.43	-11.88	541.4	542.4	-
Fm	600.2	-24.56	-3.40	-14.68	557.5	-25.13	-3.52	-14.68	556.8	557.7	-
Md	637.4	-26.40	-4.43	-39.28	567.2	-27.14	-4.42	-39.28	566.5	567.2	-
No	678.5	-28.77	-6.86	-24.68	618.2	-29.49	-7.04	-24.68	617.3	618.0	-
Lr	507.3	-7.22	0.81	2.03	502.9	-7.58	0.83	2.03	502.6	502.7	-

[i]For CM1, the ΔE_{CC} term utilized the cc-pVTZ-DK3 basis set, while the ΔE_{CV} term used the cc-pwCVDZ-DK3 basis set. In CM2, the ΔE_{CC} term utilized the cc-pVQZ-DK3 basis set, while the ΔE_{CV} term used the cc-pwCVTZ-DK3 basis set.

[ii]The error in the experimental ionization energies for the last digits is given in parentheses.

As was observed for the second ionization energies, the RMSD from the third ionization energies obtained using the CCSD(T)+DHF composite is smaller when using CM2 than when using CM1 to obtain these values (Figure 3). In fact, for the third ionization energies using CM2 instead of CM1 reduces the RMSD by more than half. The largest differences between the third ionization energies obtained using CM1 and CM2, and those obtained using the CCSD(T)+DHF method occur for Pa, U and Np.

Though the ΔE_{CC} contribution to the energy is very large (nearing ~30 kcal mol^{-1} for some elements) there is little variation in this term regardless of which composite method (CM1 or CM2) is used. For most elements in the series there is < 0.5 kcal mol^{-1} of a difference between this term obtained with CM1 and that obtained using CM2. Therefore this indicates that while the method used (CCSD(T) versus MP2) affects the ionization energy greatly, the use of a triple- or quadruple-ζ basis set is fairly inconsequential for the determination of this contribution to the energy.

Examining the ΔE_{CV} term obtained using CM1 and CM2 for the third ionization energy, the range of values between the two composites is not as large as for the second ionization energies. The largest difference in terms occurs for Pa (ΔE_{CV}=-5.8 kcal mol^{-1} using CM1 and -1.1 kcal mol^{-1} using CM2). The terms for U are closer together, with about 2 kcal mol^{-1} difference and opposite signs. Using CM1, the ΔE_{CV} term for U is -0.69 kcal mol^{-1}, with a total third ionization energy of 446.8 kcal mol^{-1}. When using CM2, ΔE_{CV} is 1.50 kcal mol^{-1} and the total third ionization energy for U is 449.0 kcal mol^{-1}. The experimental value for the third ionization energy of uranium is 457 ± 7 kcal mol^{-1}. Therefore, the third ionization energy obtained using CM2 is < 1 kcal mol^{-1} below the lower bound of the experimental value (450-464 kcal mol^{-1}). Previous

theoretical work done using MRCI+Q/FPD[61] and CASSCF/MRACPF-PP[76] gave a third ionization energy for this element of 435.38 kcal mol^{-1} and 433.5 kcal mol^{-1}, respectively. Thus either composite in this work offers a significant improvement in accuracy for uranium's third ionization energy, using only single-reference methods, at a significantly reduced computational cost when compared to multi-reference methods.

There are differences of ~1.5 kcal mol^{-1} for Np and Pu between terms obtained using CM1 and CM2. The differences between terms obtained using CM1 and CM2 are far smaller for the remaining elements (less than 1 kcal mol^{-1}, and even far below 0.5 kcal mol^{-1} in some cases).

While the ΔE_{CV} term for thorium is fairly consistent regardless of whether CM1 (ΔE_{CV} = -0.92 kcal mol^{-1}) or CM2 (ΔE_{CV} = -0.80 kcal mol^{-1}) is used, this term is quite a bit smaller in magnitude than the CBS extrapolated value found using MRCI+Q/FPD[61] (-3.37 kcal mol^{-1}). However, the total third ionization energy for thorium found using either CM1 or CM2 is ~4 kcal mol^{-1} *below* the lower bound of the experimental error range, at 417.0 and 417.1 kcal mol^{-1}, respectively. Therefore it may be the positive ΔE_{CC} contribution that is lacking in this case. This indicates that even the use of a quadruple-ζ basis set is not sufficient for recovery of the post-HF correlation energy for this element; correct recovery of this term may require a multireference treatment.

To further compare the α-ccCA performance to that of the CCSD(T)+DHF composite with CBS extrapolation, the total times required for CM1 and CM2 are 24% and 60% that of the CCSD(T)+DHF composite scheme, respectively. Table S1 in the SI shows the percentages of the total time for each step for the three composite methods when used to obtain the total energy for actinium (Ac), as well as the number of basis functions used. The bottleneck for CPU time for both CM1 and CM2 is in calculating the CCSD(T) energy and considering only the valence electrons active, for use in obtaining the core-core and core-valence term (using the cc-pwCVDZ-DK3 and cc-pwCVTZ-DK3 basis sets, respectively). For the CCSD(T)+DHF total energy calculation the time required for each step increases monotonically with the number of basis functions used.

Conclusions

The first, second, and third ionization energies have been obtained using the CCSD(T)+DHF method. This method offers an improvement in accuracy for theoretically determined ionization energies at a decreased computational cost as compared to more costly multireference methods. The overall RMSD of the CBS extrapolated (valence and outer-core electrons correlated, cc-pwCV*n*Z-DK3 basis set) first ionization energies from experimental data for the series is 0.38 kcal mol^{-1}; multireference methods resulted in RMSD's relative to experiment of 5.59 kcal mol^{-1} [61] and 6.67 kcal mol^{-1} [76].

Additionally, for the first time, a correlation-consistent composite approach (α-ccCA), has been implemented for calculating ionization potentials for the actinide series. For the first ionization energies, the RMSD with respect to experiment obtained using the α-ccCA is 1.85 kcal mol^{-1}. Additionally, this method is significantly less computationally expensive than the single-reference CCSD(T)+DHF /CBS method (as illustrated for the first ionization energy of actinium, where the total times required for CM1 and CM2 (two variants of the α-ccCA) are 24% and 60% that of the CCSD(T)+DHF/CBS composite, respectively).

The second and third ionization potentials are compared to experimental values where (sparingly) available. For the elements actinium and uranium, second ionization energies obtained are within error limits of the experimental values. The α-ccCA method is found to give a value for the second ionization energy of thorium that is ~4 kcal mol^{-1} above the upper limit of experimental error; this is due to insufficient recovery of core-core and core-valence interactions. As a whole, the second ionization energies have a RMSD from the CCSD(T)+DHF composite values of below 1.50 kcal mol^{-1} when CM2 is used.

For the third ionization energies, the closest value to experiment for thorium obtained with the α-ccCA is ~4 kcal mol^{-1} below the lower limit of the experimental value when CM2 is used. The α-ccCA does much better when obtaining the third ionization energy of uranium, ~1 kcal mol^{-1} below the lower limit of the experimental uncertainty. Taken together, the third ionization energies have a RMSD from the simple composite values of just 1.03 kcal mol^{-1} when CM2 is used.

Acknowledgements
This material is based upon work supported by the National Science Foundation under Grant No. CHE-1900086. This work also utilized computational facilities at the Institute for Cyber-Enabled Research (ICER) at Michigan State University.

References

(1) Greenwood, N. N.; Earnshaw, A. *Chemistry of The Elements*, 2nd ed.; Butterworth-Heinemann: Waltham, Massachusetts, 1997.
(2) Jacobson, M. Z. *100% Clean, Renewable Energy and Storage for Everything*; Cambridge University Press: Cambridge, UK.
(3) Sovacool, B. K. Valuing the Greenhouse Gas Emissions from Nuclear Power: A Critical Survey. *Energy Policy* **2008**, *36* (8), 2950–2963. https://doi.org/10.1016/j.enpol.2008.04.017.
(4) Lee, S.; Kim, M.; Lee, J. Analyzing the Impact of Nuclear Power on CO2 Emissions. *Sustain.* **2017**, *9* (8), 1–13. https://doi.org/10.3390/su9081428.
(5) Fitzsimmons, J.; Atcher, R. Synthesis and Evaluation of a Water-Soluble Polymer to Reduce Ac-225 Daughter Migration. *J. Label. Compd. Radiopharm.* **2007**, *50* (2), 147–153. https://doi.org/10.1002/jlcr.1143.
(6) Fitzsimmons, J.; Foley, B.; Torre, B.; Wilken, M.; Cutler, C. S.; Mausner, L.; Medvedev, D. Optimization of Cation Exchange for the Separation of Actinium-225 from Radioactive Thorium, Radium-223 and Other Metals. *Molecules* **2019**, *24* (10). https://doi.org/10.3390/molecules24101921.
(7) Thiele, N. A.; Brown, V.; Kelly, J. M.; Amor-Coarasa, A.; Jermilova, U.; MacMillan, S. N.; Nikolopoulou, A.; Ponnala, S.; Ramogida, C. F.; Robertson, A. K. H.; Rodríguez-Rodríguez, C.; Schaffer, P.; Williams, C.; Babich, J. W.; Radchenko, V.; Wilson, J. J. An Eighteen-Membered Macrocyclic Ligand for Actinium-225 Targeted Alpha Therapy. *Angew. Chemie - Int. Ed.* **2017**, *56* (46), 14712–14717. https://doi.org/10.1002/anie.201709532.
(8) Reisinger, K. S. Smoke Detectors: Reducing Deaths and Injuries Due to Fire. *Pediatrics* **1980**, *65* (4), 718–724.
(9) Kaltsoyannis, N. Transuranic Computational Chemistry. *Chemistry - A European Journal*. Wiley-VCH Verlag February 26, 2018, pp 2815–2825. https://doi.org/10.1002/chem.201704445.
(10) Seaborg, G. T. No Title. *Nucl. Sci. Eng.* **1961**, *9*, 475–487.
(11) Brown, J. L.; Batista, E. R.; Boncella, J. M.; Gaunt, A. J.; Reilly, S. D.; Scott, B. L.; Tomson, N. C. A Linear Trans-Bis(Imido) Neptunium(V) Actinyl Analog: NpV(NDipp)2(TBu2bipy)2Cl

(Dipp = 2,6-IPr2C6H3). *J. Am. Chem. Soc.* **2015**, *137* (30), 9583–9586. https://doi.org/10.1021/jacs.5b06667.
(12) Arnold, P. L.; Dutkiewicz, M. S.; Zegke, M.; Walter, O.; Apostolidis, C.; Hollis, E.; Pécharman, A. F.; Magnani, N.; Griveau, J. C.; Colineau, E.; Caciuffo, R.; Zhang, X.; Schreckenbach, G.; Love, J. B. Subtle Interactions and Electron Transfer between UIII, NpIII, or PuIIIand Uranyl Mediated by the Oxo Group. *Angew. Chemie - Int. Ed.* **2016**, *55* (41), 12797–12801. https://doi.org/10.1002/anie.201607022.
(13) Silver, M. A.; Cary, S. K.; Johnson, J. A.; Baumbach, R. E.; Arico, A. A.; Luckey, M.; Urban, M.; Wang, J. C.; Polinski, M. J.; Chemey, A.; Liu, G.; Chen, K. W.; Van Cleve, S. M.; Marsh, M. L.; Eaton, T. M.; Van De Burgt, L. J.; Gray, A. L.; Hobart, D. E.; Hanson, K.; Maron, L.; Gendron, F.; Autschbach, J.; Speldrich, M.; Kögerler, P.; Yang, P.; Braley, J.; Albrecht-Schmitt, T. E. Characterization of Berkelium(III) Dipicolinate and Borate Compounds in Solution and the Solid State. *Science (80-.).* **2016**, *353* (6302). https://doi.org/10.1126/science.aaf3762.
(14) Deblonde, G. J. P.; Sturzbecher-Hoehne, M.; Rupert, P. B.; An, D. D.; Illy, M. C.; Ralston, C. Y.; Brabec, J.; De Jong, W. A.; Strong, R. K.; Abergel, R. J. Chelation and Stabilization of Berkelium in Oxidation State +IV. *Nat. Chem.* **2017**, *9* (9), 843–849. https://doi.org/10.1038/nchem.2759.
(15) Hohenburg, P.; Kohn, W. No Title. *Phys. Rev.* **1964**, *136*, B864.
(16) Burke, K. arXiv:1201.3679 [physics.chem-ph].
(17) Carrascal, D. J.; Ferrer, J.; Smith, J. C.; Burke, K. The Hubbard Dimer: A Density Functional Case Study of a Many-Body Problem. *J. Phys. Condens. Matter* **2015**, *27* (39), 393001. https://doi.org/10.1088/0953-8984/27/39/393001.
(18) Cohen, A. J.; Mori-Sánchez, P.; Yang, W. Insights into Current Limitations of Density Functional Theory. *Science*. August 8, 2008, pp 792–794. https://doi.org/10.1126/science.1158722.
(19) Chai, J. Da. Density Functional Theory with Fractional Orbital Occupations. *J. Chem. Phys.* **2012**, *136* (15). https://doi.org/10.1063/1.3703894.
(20) Chai, J. Da. Thermally-Assisted-Occupation Density Functional Theory with Generalized-Gradient Approximations. *J. Chem. Phys.* **2014**, *140* (18). https://doi.org/10.1063/1.4867532.
(21) Chen, Z.; Zhang, D.; Jin, Y.; Yang, Y.; Su, N. Q.; Yang, W. Multireference Density Functional Theory with Generalized Auxiliary Systems for Ground and Excited States. *J. Phys. Chem. Lett.* **2017**, *8* (18), 4479–4485. https://doi.org/10.1021/acs.jpclett.7b01864.
(22) Chai, J. Da. Role of Exact Exchange in Thermally-Assisted-Occupation Density Functional Theory: A Proposal of New Hybrid Schemes. *J. Chem. Phys.* **2017**, *146* (4). https://doi.org/10.1063/1.4974163.
(23) Becke, A. D.; Roussel, M. R. Exchange Holes in Inhomogeneous Systems: A Coordinate-Space Model. *Phys. Rev. A* **1989**, *39* (8), 3761–3767. https://doi.org/10.1103/PhysRevA.39.3761.
(24) Becke, A. D. A Real-Space Model of Nondynamical Correlation. *J. Chem. Phys.* **2003**, *119* (6), 2972–2977. https://doi.org/10.1063/1.1589733.
(25) Becke, A. D. Real-Space Post-Hartree-Fock Correlation Models. *J. Chem. Phys.* **2005**, *122* (6). https://doi.org/10.1063/1.1844493.
(26) Becke, A. D. Density Functionals for Static, Dynamical, and Strong Correlation. *J. Chem. Phys.* **2013**, *138* (7). https://doi.org/10.1063/1.4790598.
(27) Laqua, H.; Kussmann, J.; Ochsenfeld, C. Communication: Density Functional Theory Model for Multi-Reference Systems Based on the Exact-Exchange Hole Normalization. *J. Chem. Phys.* **2018**, *148* (12). https://doi.org/10.1063/1.5025334.
(28) Grimme, S.; Waletzke, M. A Combination of Kohn-Sham Density Functional Theory and Multi-Reference Configuration Interaction Methods. *J. Chem. Phys.* **1999**, *111* (13), 5645–5655.

https://doi.org/10.1063/1.479866.
(29) Escudero, D.; Thiel, W. Assessing the Density Functional Theory-Based Multireference Configuration Interaction (DFT/MRCI) Method for Transition Metal Complexes. *J. Chem. Phys.* **2014**, *140* (19). https://doi.org/10.1063/1.4875810.
(30) Shamasundar, K. R.; Knizia, G.; Werner, H. J. A New Internally Contracted Multi-Reference Configuration Interaction Method. *J. Chem. Phys.* **2011**, *135* (5). https://doi.org/10.1063/1.3609809.
(31) Pople, J. A.; Head-Gordon, M.; Fox, D. J.; Raghavachari, K.; Curtiss, L. A. Gaussian-1 Theory: A General Procedure for Prediction of Molecular Energies. *J. Chem. Phys.* **1989**, *90* (10), 5622–5629. https://doi.org/10.1063/1.456415.
(32) Curtiss, L. A.; Jones, C.; Trucks, G. W.; Raghavachari, K.; Pople, J. A. Gaussian-1 Theory of Molecular Energies for Second-Row Compounds. *J. Chem. Phys.* **1990**, *93* (4), 2537–2545. https://doi.org/10.1063/1.458892.
(33) Curtiss, L. A.; Raghavachari, K.; Trucks, G. W.; Pople, J. A. Gaussian-2 Theory for Molecular Energies of First- and Second-Row Compounds. *J. Chem. Phys.* **1991**, *94* (11), 7221–7230. https://doi.org/10.1063/1.460205.
(34) Curtiss, L. A.; Raghavach Ari, K.; Redfern, P. C.; Rassolov, V.; Pople, J. A. Gaussian-3 (G3) Theory for Molecules Containing First and Second-Row Atoms. *J. Chem. Phys.* **1998**, *109* (18), 7764–7776. https://doi.org/10.1063/1.477422.
(35) Curtiss, L. A.; Redfern, P. C.; Raghavachari, K.; Pople, J. A. Gaussian-3X (G3X) Theory: Use of Improved Geometries, Zero-Point Energies, and Hartree-Fock Basis Sets. *J. Chem. Phys.* **2001**, *114* (1), 108–117. https://doi.org/10.1063/1.1321305.
(36) Curtiss, L. A.; Redfern, P. C.; Raghavachari, K. Gaussian-4 Theory. *J. Chem. Phys.* **2007**, *126* (8). https://doi.org/10.1063/1.2436888.
(37) Martin, J. M. L.; De Oliveira, G. Towards Standard Methods for Benchmark Quality Ab Initio Thermochemistry - W1 and W2 Theory. *J. Chem. Phys.* **1999**, *111* (5), 1843–1856. https://doi.org/10.1063/1.479454.
(38) Parthiban, S.; Martin, J. M. L. Assessment of W1 and W2 Theories for the Computational of Electron Affinities, Ionization Potentials, Heats of Formation, and Proton Affinities. *J. Chem. Phys.* **2001**, *114* (14), 6014–6029. https://doi.org/10.1063/1.1356014.
(39) Daniel Boese, A.; Oren, M.; Atasoylu, O.; Martin, J. M. L.; Kállay, M.; Gauss, J. W3 Theory: Robust Computational Thermochemistry in the KJ/Mol Accuracy Range. *J. Chem. Phys.* **2004**, *120* (9), 4129–4141. https://doi.org/10.1063/1.1638736.
(40) Karton, A.; Rabinovich, E.; Martin, J. M. L.; Ruscic, B. W4 Theory for Computational Thermochemistry: In Pursuit of Confident Sub-KJ/Mol Predictions. *J. Chem. Phys.* **2006**, *125* (14), 144108. https://doi.org/10.1063/1.2348881.
(41) Petersson, G. A.; Bennett, A.; Tensfeldt, T. G.; Al-Laham, M. A.; Shirley, W. A.; Mantzaris, J. A Complete Basis Set Model Chemistry. I. The Total Energies of Closed-Shell Atoms and Hydrides of the First-Row Elements. *J. Chem. Phys.* **1988**, *89* (4), 2193–2218. https://doi.org/10.1063/1.455064.
(42) Petersson, G. A.; Tensfeldt, T. G.; Montgomery, J. A. A Complete Basis Set Model Chemistry. III. The Complete Basis Set-Quadratic Configuration Interaction Family of Methods. *J. Chem. Phys.* **1991**, *94* (9), 6091–6101. https://doi.org/10.1063/1.460448.
(43) Petersson, G. A.; Al-Laham, M. A. A Complete Basis Set Model Chemistry. II. Open-Shell Systems and the Total Energies of the First-Row Atoms. *J. Chem. Phys.* **1991**, *94* (9), 6081–6090. https://doi.org/10.1063/1.460447.

(44) Ochterski, J. W.; Petersson, G. A.; Montgomery, J. A. A Complete Basis Set Model Chemistry. V. Extensions to Six or More Heavy Atoms. *J. Chem. Phys.* **1996**, *104* (7), 2598–2619. https://doi.org/10.1063/1.470985.
(45) Montgomery, J. A.; Ochterski, J. W.; Petersson, G. A. A Complete Basis Set Model Chemistry. IV. An Improved Atomic Pair Natural Orbital Method. *J. Chem. Phys.* **1994**, *101* (7), 5900–5909. https://doi.org/10.1063/1.467306.
(46) Montgomery, J. A.; Frisch, M. J.; Ochterski, J. W.; Petersson, G. A. A Complete Basis Set Model Chemistry. VI. Use of Density Functional Geometries and Frequencies. *J. Chem. Phys.* **1999**, *110* (2–12), 2822–2827. https://doi.org/10.1063/1.477924.
(47) Tajti, A.; Szalay, P. G.; Császár, A. G.; Kállay, M.; Gauss, J.; Valeev, E. F.; Flowers, B. A.; Vázquez, J.; Stanton, J. F. HEAT: High Accuracy Extrapolated Ab Initio Thermochemistry. *J. Chem. Phys.* **2004**, *121* (23), 11599–11613. https://doi.org/10.1063/1.1811608.
(48) Bomble, Y. J.; Vázquez, J.; Kállay, M.; Michauk, C.; Szalay, P. G.; Császár, A. G.; Gauss, J.; Stanton, J. F. High-Accuracy Extrapolated Ab Initio Thermochemistry. II. Minor Improvements to the Protocol and a Vital Simplification. *J. Chem. Phys.* **2006**, *125* (6). https://doi.org/10.1063/1.2206789.
(49) Feller, D.; Peterson, K. A.; Dixon, D. A. No Title. *J. Chem. Phys.* **2008**, *129*, 204105.
(50) Peterson, K. A.; Feller, D.; Dixon, D. A. No Title. *Theor. Chem. Acc.* **2012**, *131*, 1079.
(51) Dixon, D. A.; Feller, D.; Peterson, K. A. No Title. *Annu. Rep. Comput. Chem.* **2012**, *8*, 1.
(52) DeYonker, N. J.; Cundari, T. R.; Wilson, A. K. The Correlation Consistent Composite Approach (CcCA): An Alternative to the Gaussian-n Methods. *J. Chem. Phys.* **2006**, *124* (11). https://doi.org/10.1063/1.2173988.
(53) DeYonker, N. J.; Grimes, T.; Yockel, S.; Dinescu, A.; Mintz, B.; Cundari, T. R.; Wilson, A. K. The Correlation-Consistent Composite Approach: Application to the G3/99 Test Set. *J. Chem. Phys.* **2006**, *125* (10). https://doi.org/10.1063/1.2236116.
(54) DeYonker, N. J.; Ho, D. S.; Wilson, A. K.; Cundari, T. R. Computational S-Block Thermochemistry with the Correlation Consistent Composite Approach. *J. Phys. Chem. A* **2007**, *111* (42), 10776–10780. https://doi.org/10.1021/jp0736241.
(55) DeYonker, N. J.; Mintz, B.; Cundari, T. R.; Wilson, A. K. Application of the Correlation Consistent Composite Approach (CcCA) to Third-Row (Ga-Kr) Molecules. *J. Chem. Theory Comput.* **2008**, *4* (2), 328–334. https://doi.org/10.1021/ct7002463.
(56) DeYonker, N. J.; Peterson, K. A.; Steyl, G.; Wilson, A. K.; Cundari, T. R. Quantitative Computational Thermochemistry of Transition Metal Species. *J. Phys. Chem. A* **2007**, *111* (44), 11269–11277. https://doi.org/10.1021/jp0715023.
(57) Deyonker, N. J.; Williams, T. G.; Imel, A. E.; Cundari, T. R.; Wilson, A. K. Accurate Thermochemistry for Transition Metal Complexes from First-Principles Calculations. *J. Chem. Phys.* **2009**, *131* (2). https://doi.org/10.1063/1.3160667.
(58) Jiang, W.; Deyonker, N. J.; Determan, J. J.; Wilson, A. K. Toward Accurate Theoretical Thermochemistry of First Row Transition Metal Complexes. *J. Phys. Chem. A* **2012**, *116* (2), 870–885. https://doi.org/10.1021/jp205710e.
(59) Weber, R.; Wilson, A. K. Do Composite Methods Achieve Their Target Accuracy? *Comput. Theor. Chem.* **2015**, *1072*, 58–62. https://doi.org/10.1016/j.comptc.2015.08.015.
(60) Peterson, K. A. Correlation Consistent Basis Sets for Actinides. I. the Th and U Atoms. *J. Chem. Phys.* **2015**, *142* (7). https://doi.org/10.1063/1.4907596.
(61) Feng, R.; Peterson, K. A. Correlation Consistent Basis Sets for Actinides. II. the Atoms Ac and Np-Lr. *J. Chem. Phys.* **2017**, *147* (8). https://doi.org/10.1063/1.4994725.

(62) Wang, S. G.; Pan, D. K.; Schwarz, W. H. E. Density Functional Calculations of Lanthanide Oxides. *J. Chem. Phys.* **1995**, *102* (23), 9296–9308. https://doi.org/10.1063/1.468796.
(63) Meng, J. H.; Zhao, Y. X.; He, S. G. Reactivity of Stoichiometric Lanthanum Oxide Cluster Cations in C-H Bond Activation. *J. Phys. Chem. C* **2013**, *117* (34), 17548–17556. https://doi.org/10.1021/jp4039286.
(64) Maron, L.; Eisenstein, O. Do f Electrons Play a Role in the Lanthanide-Ligand Bonds? A DFT Study of Ln(NR2)3; R = H, SiH3. *J. Phys. Chem. A* **2000**, *104* (30), 7140–7143. https://doi.org/10.1021/jp0010278.
(65) Luo, Y.; Wan, X.; Ito, Y.; Takami, S.; Kubo, M.; Miyamoto, A. A Density Functional Theory Calculation on Lanthanide Monosulfides. *Chem. Phys.* **2002**, *282* (2), 197–206. https://doi.org/10.1016/S0301-0104(02)00716-4.
(66) Hargittai, M. Molecular Structure of Metal Halides. *Chem. Rev.* **2000**, *100* (6), 2233–2301. https://doi.org/10.1021/cr970115u.
(67) Aebersold, L. E.; Wilson, A. K. Considering Density Functional Approaches for Actinide Species: The An66 Molecule Set. *J. Phys. Chem. A* **2021**, *125* (32), 7029–7037. https://doi.org/10.1021/acs.jpca.1c06155.
(68) Grimmel, S.; Schoendorff, G.; Wilson, A. K. Gauging the Performance of Density Functionals for Lanthanide-Containing Molecules. *J. Chem. Theory Comput.* **2016**, *12* (3), 1259–1266. https://doi.org/10.1021/acs.jctc.5b01193.
(69) Aebersold, L. E.; Yuwono, S. H.; Schoendorff, G.; Wilson, A. K. Efficacy of Density Functionals and Relativistic Effective Core Potentials for Lanthanide-Containing Species: The Ln54 Molecule Set. *J. Chem. Theory Comput.* **2017**, *13* (6), 2831–2839. https://doi.org/10.1021/acs.jctc.6b01223.
(70) Ren, C. Y. Relativistic Density-Functional All-Electron Calculations of Interconfigurational Energies of Lanthanide Atoms. *J. Chem. Phys.* **2004**, *121* (22), 11073–11082. https://doi.org/10.1063/1.1814931.
(71) Liu, W.; Dolg, M. Benchmark Calculations for Lanthanide Atoms: Calibration of Ab Initio and Density-Functional Methods. *Phys. Rev. A - At. Mol. Opt. Phys.* **1998**, *57* (3), 1721–1728. https://doi.org/10.1103/PhysRevA.57.1721.
(72) Cao, X.; Dolg, M. Valence Basis Sets for Relativistic Energy-Consistent Small-Core Lanthanide Pseudopotentials. *J. Chem. Phys.* **2001**, *115* (16), 7348–7355. https://doi.org/10.1063/1.1406535.
(73) Cao, X.; Dolg, M. Basis Set Limit Extrapolation of ACPF and CCSD(T) Results for the Third and Fourth Lanthanide Ionization Potentials. *Chem. Phys. Lett.* **2001**, *349* (5–6), 489–495. https://doi.org/10.1016/S0009-2614(01)01211-8.
(74) Piecuch, P.; Kucharski, S. A.; Kowalski, K.; Musiał, M. Efficient Computer Implementation of the Renormalized Coupled-Cluster Methods: The R-CCSD[T], R-CCSD(T), CR-CCSD[T], and CR-CCSD(T) Approaches. *Comput. Phys. Commun.* **2002**, *149* (2), 71–96. https://doi.org/10.1016/S0010-4655(02)00598-2.
(75) Peterson, C.; Penchoff, D. A.; Wilson, A. K. Ab Initio Approaches for the Determination of Heavy Element Energetics: Ionization Energies of Trivalent Lanthanides (Ln = La-Eu). *J. Chem. Phys.* **2015**, *143* (19). https://doi.org/10.1063/1.4935809.
(76) Cao, X.; Dolg, M. Theoretical Prediction of the Second to Fourth Actinide Ionization Potentials. *Mol. Phys.* **2003**, *101* (7), 961–969. https://doi.org/10.1080/0026897021000046807.
(77) Küchle, W.; Dolg, M.; Stoll, H.; Preuss, H. Energy-Adjusted Pseudopotentials for the Actinides. Parameter Sets and Test Calculations for Thorium and Thorium Monoxide. *J. Chem. Phys.* **1994**, *100* (10), 7535–7542. https://doi.org/10.1063/1.466847.
(78) Cao, X.; Dolg, M.; Stoll, H. Valence Basis Sets for Relativistic Energy-Consistent Small-Core

Actinide Pseudopotentials. *J. Chem. Phys.* **2003**, *118* (2), 487–496. https://doi.org/10.1063/1.1521431.
(79) Reiher, M.; Wolf, A. Exact Decoupling of the Dirac Hamiltonian. I. General Theory. *J. Chem. Phys.* **2004**, *121* (5), 2037–2047. https://doi.org/10.1063/1.1768160.
(80) Dyall, K. G. An Exact Separation of the Spin-Free and Spin-Dependent Terms of the Dirac-Coulomb-Breit Hamiltonian. *J. Chem. Phys.* **1994**, *100* (3), 2118–2127. https://doi.org/10.1063/1.466508.
(81) Thyssen, J. PhD Dissertation, University of Southern Denmark, 2001.
(82) Gomes, A. S. .; Saue, T.; Visscher, L.; Jensen, H. J. A.; Bast, R. DIRAC, a Relativistic Ab Initio Electronic Structure Program. 2019.
(83) Dyall, K. G. Relativistic Double-Zeta, Triple-Zeta, and Quadruple-Zeta Basis Sets for the Actinides Ac-Lr. *Theor. Chem. Acc.* **2007**, *117* (4), 491–500. https://doi.org/10.1007/s00214-006-0175-4.
(84) Visser, O.; Visscher, L.; Aerts, P. J. C.; Nieuwpoor, W. C. Molecular Open Shell Configuration Interaction Calculations Using the Dirac-Coulomb Hamiltonian: The F6-Manifold of an Embedded EuO 69- Cluster. *J. Chem. Phys.* **1992**, *96* (4), 2910–2919. https://doi.org/10.1063/1.461987.
(85) Halkier, A.; Helgaker, T.; Jørgensen, P.; Klopper, W.; Olsen, J. Basis-Set Convergence of the Energy in Molecular Hartree-Fock Calculations. *Chem. Phys. Lett.* **1999**, *302* (5–6), 437–446. https://doi.org/10.1016/S0009-2614(99)00179-7.
(86) Feller, D. Application of Systematic Sequences of Wave Functions to the Water Dimer. *J. Chem. Phys.* **1992**, *96* (8), 6104–6114. https://doi.org/10.1063/1.462652.
(87) Feller, D. The Use of Systematic Sequences of Wave Functions for Estimating the Complete Basis Set, Full Configuration Interaction Limit in Water. *J. Chem. Phys.* **1993**, *98* (9), 7059–7071. https://doi.org/10.1063/1.464749.
(88) Williams, T. G.; Deyonker, N. J.; Wilson, A. K. Hartree-Fock Complete Basis Set Limit Properties for Transition Metal Diatomics. *J. Chem. Phys.* **2008**, *128* (4). https://doi.org/10.1063/1.2822907.
(89) Martin, J. M. L. Ab Initio Total Atomization Energies of Small Molecules - Towards the Basis Set Limit. *Chem. Phys. Lett.* **1996**, *259* (5–6), 669–678. https://doi.org/10.1016/0009-2614(96)00898-6.
(90) Feller, D.; Peterson, K. A.; Grant Hill, J. On the Effectiveness of CCSD(T) Complete Basis Set Extrapolations for Atomization Energies. *J. Chem. Phys.* **2011**, *135* (4). https://doi.org/10.1063/1.3613639.
(91) Møller, C.; Plesset, M. S. Note on an Approximation Treatment for Many-Electron Systems. *Phys. Rev.* **1934**, *46* (7), 618–622. https://doi.org/10.1103/PhysRev.46.618.
(92) Karton, A.; Martin, J. M. L. Comment on: "Estimating the Hartree-Fock Limit from Finite Basis Set Calculations" [Jensen F (2005) Theor Chem Acc 113:267]. *Theor. Chem. Acc.* **2006**, *115* (4), 330–333. https://doi.org/10.1007/s00214-005-0028-6.
(93) Peterson, K. A.; Woon, D. E.; Dunning, T. H. Benchmark Calculations with Correlated Molecular Wave Functions. IV. The Classical Barrier Height of the H+H2→H2+H Reaction. *J. Chem. Phys.* **1994**, *100* (10), 7410–7415. https://doi.org/10.1063/1.466884.
(94) Werner, H. J.; Knowles, P. J.; Knizia, G.; Manby, F. R.; Schutz, M.; Al., E. MOLPRO, Version 2010.1, a Package of Ab Initio Programs, 2010, See Http://Www.Molpro.Net.
(95) T.~Saue; L.~Visscher; H.~J.~{\relax Aa}.~Jensen, R. ~Bas.; V.~Bakken; K.~G.~Dyall; S.~Dubillard; U.~Ekstr{\"o}m; E.~Eliav; T.~Enevoldsen; E.~Fa{\ss}hauer; T.~Fleig; O.~Fossgaard, A. ~S. ~P. ~Gome.; E.~D.~Hedeg{\aa}rd, T. ~Helgake.; J.~Henriksson;

M.~Ilia{\v{s}}; Ch.~R.~Jacob; S.~Knecht; S.~Komorovsk{\'y}; O.~Kullie; J.~K.~L{\ae}rdahl, C. ~V. ~Larse.; Y.~S.~Lee; H.~S.~Nataraj; M.~K.~Nayak; P.~Norman; G.~Olejniczak; J.~Olsen; J.~M.~H.~Olsen; Y.~C.~Park; J.~K.~Pedersen, M.~Pernpointner, R. ~di~Remigi.; K.~Ruud; P.~Sa{\l}ek, B. ~Schimmelpfenni.; A.~Shee; J.~Sikkema, A.~J.~Thorvaldsen, J. ~Thysse.; J.~van~Stralen; S.~Villaume; O.~Visser; T.~Winther; S.~Yamamoto. DIRAC, a Relativistic Ab Initio Electronic Structure Program. 2019. https://doi.org/http://dx.doi.org/10.5281/zenodo.3572669.

(96) Dolg, M. *The Encyclopedia of Computational Chemistry*; Schleyer, P. v. R., N. L. Allinger, T. Clark, J. Gasteiger, P. A. Kollman, H. F. S. 111 and P. R., Schreiner, Eds.; Wiley: Chichester, 1998.

(97) A. Kramida, Yu. Ralchenko, J. Reader, and NIST ASD Team NIST Atomic Spectra Database (ver. 5.7.1), [Online], available: http://physics.nist.gov/asd, Wed Aug 26 2020, National Institute of Standards and Technology, Gaithersburg, MD, 2014.

(98) Roßnagel, J.; Raeder, S.; Hakimi, A.; Ferrer, R.; Trautmann, N.; Wendt, K. Determination of the First Ionization Potential of Actinium. *Phys. Rev. A - At. Mol. Opt. Phys.* **2012**, *85* (1). https://doi.org/10.1103/PhysRevA.85.012525.

(99) Waldek, A.; Erdmann, N.; Gruening, C.; Huber, G.; Kunz, P.; Kratz, J.; Lassen, J.; Passler, G.; Trautmann, N. No Title. *AIP Conf. Proc.* **2001**, *584*, 219.

(100) Köhler, S.; Deißenberger, R.; Eberhardt, K.; Erdmann, N.; Herrmann, G.; Huber, G.; Kratz, J. V.; Nunnemann, M.; Passler, G.; Rao, P. M.; Riegel, J.; Trautmann, N.; Wendt, K. Determination of the First Ionization Potential of Actinide Elements by Resonance Ionization Mass Spectroscopy. *Spectrochim. Acta - Part B At. Spectrosc.* **1997**, *52* (6 PART B), 717–726. https://doi.org/10.1016/s0584-8547(96)01670-9.

(101) Sugar, J. Revised Ionization Energies of the Neutral Actinides. *The Journal of Chemical Physics*. 1974, p 4103. https://doi.org/10.1063/1.1680874.

(102) Coste, A.; Avril, R.; Blancard, P.; Chatelet, J.; Lambert, D.; Legre, J.; Liberman, S.; Pinard, J. NEW SPECTROSCOPIC DATA ON HIGH-LYING EXCITED LEVELS OF ATOMIC URANIUM. *J. Opt. Soc. Am.* **1982**, *72* (1), 103–109. https://doi.org/10.1364/JOSA.72.000103.

(103) Chhetri, P.; Ackermann, D.; Backe, H.; Block, M.; Cheal, B.; Droese, C.; Düllmann, C. E.; Even, J.; Ferrer, R.; Giacoppo, F.; Götz, S.; Heßberger, F. P.; Huyse, M.; Kaleja, O.; Khuyagbaatar, J.; Kunz, P.; Laatiaoui, M.; Lautenschläger, F.; Lauth, W.; Lecesne, N.; Lens, L.; Minaya Ramirez, E.; Mistry, A. K.; Raeder, S.; Van Duppen, P.; Walther, T.; Yakushev, A.; Zhang, Z. Precision Measurement of the First Ionization Potential of Nobelium. *Phys. Rev. Lett.* **2018**, *120* (26). https://doi.org/10.1103/PhysRevLett.120.263003.

(104) Sato, T. K.; Asai, M.; Borschevsky, A.; Stora, T.; Sato, N.; Kaneya, Y.; Tsukada, K.; Düllmann, C. E.; Eberhardt, K.; Eliav, E.; Ichikawa, S.; Kaldor, U.; Kratz, J. V.; Miyashita, S.; Nagame, Y.; Ooe, K.; Osa, A.; Renisch, D.; Runke, J.; Schädel, M.; Thörle-Pospiech, P.; Toyoshima, A.; Trautmann, N. Measurement of the First Ionization Potential of Lawrencium, Element 103. *Nature* **2015**, *520* (7546), 209–211. https://doi.org/10.1038/nature14342.

(105) Martin, W. C.; Hagan, L.; Reader, J.; Sugar, J. No Title. *J. Phys. Chem. Ref. Data* **1974**, *3*, 771–780.

(106) Herrera-Sancho, O. A.; Nemitz, N.; Okhapkin, M. V.; Peik, E. Energy Levels of Th+ between 7.3 and 8.3 EV. *Phys. Rev. A - At. Mol. Opt. Phys.* **2013**, *88* (1). https://doi.org/10.1103/PhysRevA.88.012512.

(107) Cox, R. M.; Citir, M.; Armentrout, P. B.; Battey, S. R.; Peterson, K. A. Bond Energies of ThO + and ThC + : A Guided Ion Beam and Quantum Chemical Investigation of the Reactions of

Thorium Cation with O 2 and CO. **2019**, *184309* (2016). https://doi.org/10.1063/1.4948812.
(108) Blaise, J.; Wyart, J.-F. *No Title*; Centre National de la Recherche Scientique: Paris, France, 1992; Vol. 20.
(109) Bross, D. H.; Parmar, P.; Peterson, K. A. Multireference Configuration Interaction Calculations of the First Six Ionization Potentials of the Uranium Atom. *J. Chem. Phys.* **2015**, *143*, 184308. https://doi.org/10.1063/1.4935375.
(110) Fleig, T.; Olsen, J.; Visscher, L. The Generalized Active Space Concept for the Relativistic Treatment of Electron Correlation . II . Large-Scale Configuration Interaction Implementation Based on The Generalized Active Space Concept for the Relativistic Treatment of Electron Correlation . *J. Chem. Phys.* **2003**, *119* (6), 2963. https://doi.org/10.1063/1.1590636.
(111) Fleig, T.; Jensen, H. J. A.; Olsen, J.; Visscher, L. The Generalized Active Space Concept for the Relativistic Treatment of Electron Correlation. III. Large-Scale Configuration Interaction and Multiconfiguration Self-Consistent-Field Four-Component Methods with Application to UO2. *J. Chem. Phys.* **2006**, *124*, 104106.
(112) Knecht, S.; Jensen, H. J. A.; Fleig, T. Large-Scale Parallel Configuration Interaction . II . Two- and Four-Component Double-Group General Active Space Implementation with Application to BiH Large-Scale Parallel Configuration Interaction . II . Two- and Four-Component Double-Group General Activ. *J. Chem. Phys.* **2010**, *132*, 014108. https://doi.org/10.1063/1.3276157.
(113) Wyart, J. F. Extended Analysis of Doubly Ionized Thorium (Th Iii). *Phys. Scr.* **1981**, *24* (6), 941–952. https://doi.org/10.1088/0031-8949/24/6/006.
(114) Eliav, E.; Shmulyian, S.; Kaldor, U.; Ishikawa, Y. Transition Energies of Lanthanum, Actinium, and Eka-Actinium (Element 121). *J. Chem. Phys.* **1998**, *109* (10), 3954–3958. https://doi.org/10.1063/1.476995.
(115) Weigand, A.; Cao, X.; Hangele, T.; Dolg, M. Relativistic Small-Core Pseudopotentials for Actinium, Thorium, and Protactinium. *J. Phys. Chem. A* **2014**, *118* (13), 2519–2530. https://doi.org/10.1021/jp500215z.